Stephanie Grossi Roedel

PROCESSING AND CHARACTERIZATION OF GRADED MACROPOROUS LAYERS ON ZIRCONIA SUBSTRATES OBTAINED BY DIP COATING

Dissertação submetida ao Programa de Pós-Graduação em Ciência e Engenharia de Materiais da Universidade Federal de Santa Catarina para a obtenção do Grau de Mestre em Ciência e Engenharia de Materiais
Orientador: Prof. Dr.-Ing. Márcio Celso Fredel
Co-orientador: Prof. Dr. Bruno A. P. C. Henriques

Florianópolis
2017

Ficha de identificação da obra elaborada pelo autor
através do Programa de Geração Automática da Biblioteca Universitária
da UFSC.

Roedel, Stephanie Grossi
Processing and characterization of graded macroporous layers on zirconia substrates obtained by dip coating / Stephanie Grossi Roedel ; orientador, Márcio Celso Fredel; coorientador, Bruno A. P. C. Henriques,. Florianópolis, SC, 2017.

101 p.

Dissertação (mestrado) - Universidade Federal de Santa Catarina, Centro Tecnológico, Programa de Pós-Graduação em Ciência e Engenharia de Materiais.

Inclui referências.

1. Engenharia de Materiais. 2. zircônia. 3. *dip coating*. 4. camadas porosas. 5. FGM. I. Fredel, Márcio Celso. II. Henriques, Bruno A. P. C. III. Universidade Federal de Santa Catarina. Programa de Pós-Graduação em Engenharia Química. IV. Título.

Stephanie Grossi Roedel

PROCESSING AND CHARACTERIZATION OF GRADED MACROPOROUS LAYERS OF ZIRCONIA SUBSTRATES OBTAINED BY DIP COATING

Esta Dissertação foi julgada adequada para obtenção do Título de "Mestre em Ciência e Engenharia de Materiais", e aprovada em sua forma final pelo Programa de Pós-Graduação em Ciência e Engenharia de Materiais da Universidade Federal de Santa Catarina.

Florianópolis, 30 de maio de 2017.

_____
Prof. Guilherme M. O. Barra, Dr.
Coordenador – PGMAT/UFSC

_____	_____
Prof. Márcio C. Fredel, Dr.-Ing.	Prof. Bruno A. P. C. Henriques, Dr.
Orientador – EMC/UFSC	Co-orientador – UFSC/Blumenau

Banca Examinadora:

_____	_____
Prof. Dachamir Hotza, Dr.	Prof. Fernando S. Ortega, Dr.
EQA/UFSC	Centro Universitário da FEI

_____
Prof. Filipe S. Silva, Dr.
UMinho/Portugal
(Videoconferência)

Este trabalho é dedicado ao meu pai, à minha irmã, e aos queridos “roomies”, os companheiros Sabrina e Raphael.

AKNOWLEDGEMENTS

I would like to thank:

First, to my advisor Prof. Dr.-Ing. Márcio C. Fredel for the confidence, opportunities and councils, always full of knowledge.

To my co-advisor for the guidance, patience and new "insights" about research.

To Postgraduate Program in Materials Engineering (PGMAT) and CAPES for the scholarship.

To Dra. Joana M. Guimarães, for the knowledge, dedication, friendship and support.

The professor/counselor and friend Dr. Fernando S. Ortega for being the first to encourage me to do research, and for showing me the way.

To Rogerio Antonio Campos that had always facilitated the necessary bureaucratic operations, besides being always willing to help.

A heartfelt thanks to Julio and Karen Roedel for the constant support, for believing in me, for leaving your doors always open to me and all the love. Not least, thanks for Klauss Roedel and Tiago Guardia for the love and conversations full of knowledge, not to mention the joy of giving me the two cutest creatures of love.

Thanks to all friends of CERMAT, Patrícia Monich, Marcelo Barros, Useche Inchauspe, Ruben Acevedo, Thaiane Balestreri, Rafael Vidal, Veit, Lizandra Ramos, Paula Faust, among many others, for all the help and for making the work so much fun. A special thanks to Carmelita for her collaboration in the laboratory and in life.

To my UFSC friends, Lara Rebouças, Theodor van Caspel, Sérgio Yesid and Priscila Lemes, always willing to help with equipments.

To the great friends I made in Floripa, Sabrina Buziquia, Raphael Villela, Adriano Ethur, Bruna Puntel and Tobias Benitez, for being my family over there and making the moments in this city so special. Also to the ones I left in São Paulo, who supported me even from afar, giving me strength to continue my journey; you are my safe harbor.

Last but not least, to Bruno Magaldi for our fellowship, your patience and love.

I would like to thank all the people I didn't mentioned that also contributed for this journey.

Thank you!

“Simplicity is the ultimate sophistication”
(Leonardo da Vinci)

RESUMO

O presente estudo visa apresentar uma rota para obtenção de porosidade superficial em substratos de zircônia, utilizando um processo de deposição de camadas para a produção de sistemas com porosidade controlada a serem aplicados, principalmente, em próteses de zircônia. O objetivo do desenvolvimento foi mimetizar estruturas naturais, como ossos e dentes, ambos com gradientes estruturais para desempenhar diferentes papéis: estimular o crescimento de novo tecido ósseo e a osteointegração, ou atuar como interface entre componentes dissimilares. Desta forma, o objetivo principal deste estudo foi produzir um gradiente de porosidade na superfície de substratos de zircônia, através da deposição consecutiva de camadas com tamanhos de poros diferentes - obtido pelo empacotamento de partículas esféricas de diferentes tamanhos; a produção de camadas homogêneas (somente um tamanho de partículas/poros) foi necessária a fim de se otimizar cada parcela precursora do gradiente. As deposições foram feitas por *dip coating*, utilizando suspensões cerâmicas de grânulos esféricos de zircônia (Z40, Z70 e Z100 – nomeados após análise de tamanho médio de partícula, em μm) para formar diferentes porosidades. Os primeiros ensaios testaram três condições do pó Z40: não tratado, pré-sinterizado (1150ºC) e sinterizado (1500ºC); e posteriormente, a adição de partículas finas (F) ao sistema, a fim de interferir na coesão entre partículas maiores. A segunda parte dos testes considerou as outras duas camadas (Z70 e Z100), com sua relação de F otimizada, e a deposição consecutiva das três camadas para alcançar o gradiente de porosidade. A porosidade desejada foi obtida com o pó precursor pré-sinterizado, que garantiu o formato esférico das partículas durante todo o processo; a presença de F produziu pontes de ligação entre partículas grossas, aumentando a coesão das camadas, influenciando diretamente em sua resistência mecânica. O tratamento térmico entre imersões (em camadas com deposições sequenciais) foi necessário para prevenir a perda de material depositado para o meio aquoso. A presença das camadas aumentou a resistência à flexão dos substratos puros de zircônia; suas espessuras (ou o número de imersões), porém, não foram relevantes na melhoria da resistência. O gradiente de porosidade mostrou-se viável de ser produzido, com potencial para ser aplicado em próteses de zircônia, tanto para modificação superficial como para impregnação com componentes medicamentosos.

Palavras-chave: zircônia, *dip coating*, camadas porosas, FGM.

ABSTRACT

The present study was conducted to present a route to obtain surface porosity on zirconia substrates, using a layer-by-layer deposition process for the production of controlled porosity systems, to be primarily applied on zirconia prostheses. The goal of the development was to mimic natural structures, such as bones and teeth, both presenting structural gradients to perform different roles: stimulate growth of new bone tissue and/or osteointegration, or act as interface between dissimilar components. Thus, the main objective of this study was to produce a gradient of porosity on the surface of zirconia substrates through consecutive deposition of layers with different pore sizes – obtained by the packing of spherical particles of different sizes; production of homogeneous layers (only one particle/pore size) was needed in order to optimize each precursor portion of the gradient. The depositions were made by dip coating, using ceramic suspensions of zirconia spherical granules (Z40, Z70 and Z100 – named after particle size, d_{50}, in μm) to form different porosities. First tests were made with Z40 powder under three conditions: untreated, pre-sintered (1150°C) and sintered (1500°C); followed by addition of fine particles (F) to the system to investigate improvement of cohesion among large particles. The second part of the tests considered the other two layers (Z70 and Z100), with optimized F content, and the consecutive deposition of all layers to reach the porosity gradient. The desired porosity was obtained with the pre-sintered precursor powder, which ensured the spherical shape of the particles throughout the whole process; the presence of F guaranteed cohesion between coarse particles, enhancing mechanical properties of the layers. Heat treatment between immersions (on sequential deposited layers) was necessary to prevent loss of deposited material into the aqueous medium. The presence of layers increased flexural strength of pure zirconia substrates; however, its thicknesses (or number of immersions) were not relevant on the resistance improvement. The porosity gradient was feasible to be produced, with potential to be applied in zirconia prostheses, both for surface modifications and/or impregnation of medical components.

Keywords: zirconia, dip coating, porous layers, FGM.

LIST OF FIGURES

LIST OF SYMBOLS/ABREVIATIONS

YSZ – Yttria stabilized zirconia
FGM – Functionally graded materials
TBC – Thermal barrier coating
SOFC – Solid oxide fuel cell
Y-TZP – Yttria-Tetragonal zirconia polycrystals
PSZ – Partially stabilized zirconia
FSZ – Fully stabilized zirconia
LTD – Low thermal degradation
CVD – Chemical vapor deposition
SPS – Spark plasma sintering
CFC – Cubic face-centered
NT – Non-treated powders
PS – Pre-sintered powders (1150°C/1h)
S – Sintered powders (1500°C/2h)
Z3 – Zirconia powder with d_{50}= 3 μm
Z40 – Zirconia powder with d_{50}= 40 μm
Z70 – Zirconia powder with d_{50}= 70 μm
Z100 – Zirconia powder with d_{50}= 100 μm

SUMMARY

1. INTRODUCTION

The idea to produce a gradient of porosity on the surface of dense zirconia arose from the need to improve adherence between zirconia (core) and porcelain (surface) of dental crowns, which often cracks due to a weak interface. The structural function of the gradient would act for interpenetration of porcelain, to form a gradual transition of materials. To develop the gradient, a layer-by-layer technique was chosen for the advantages of good control of layer's microstructures. This concept has become attractive for its applicability in several areas and materials.

The dip coating process is effective in this procedure for its easiness, low cost and a good control on characteristics of the deposited layers. Spherical particle packing concept was used for porosity obtainment, in which the interstices form the voids of the system. The main challenge of this procedure was to optimize ceramic suspensions and powders conditions to promote the desired porosity (content and morphology of pores).

In order to reach the objective of building a gradient of porosity, were investigated the mechanical behavior and morphologies of the deposited homogeneous layers – single particle size – then, the attention was driven to the successive deposition of three (different particle sizes) homogeneous layers, ascending the order of sizes.

1.1. OBJECTIVES

In this way, the broader aim of this work was to build a gradient of porosity through successive depositions of homogeneous layers of different particle sizes, while specific aims were to obtain homogeneous porous layers of zirconia to study each one by its mechanical behavior, interconnectivity of pores and particularities.

The development of porous surfaces of zirconia over dense substrates of the same material was interesting basically for two reasons: first, for zirconia being widely used in the biomedical field, composing dental and orthopedic prostheses; and second, for rough surfaces allowing better osteointegration, besides the potential interpenetrating structure that permits its combination with a second material, forming a FGM.

1.2. STRUCTURE OF THE STUDY

The study consists of five chapters that include the present Introduction, with a broad approach to the themes addressed.

In Chapter 2, a review of literature is presented, which intends to present the properties and characteristics of biomaterials, most focused on zirconia based materials; the importance of porous structures and superficial graded porosity (FGM's); and finally, a summary of the dip coating method as a way to build the layer-by-layer structure, and how the involved forces act in the packing of particles, achieving the expected porosity.

Chapter 3 encompasses an article that focuses on the study of the required conditions to produce porous layers with the particle size of Z40 (d50 = 40 μm), and the optimized route to obtain proper cohesion and adherence of the layers.

Chapter 4 embraces the second article, which uses the studied conditions (of the previous chapter) to produce layers using other particle sizes (Z70 and Z100), and then, to apply all by successive depositions, in order to obtain gradient of porosity.

Appendix A shows the trial of different heat treatments on the interval of dipping.

Appendix B contains a few images of the porous solids produced to obtain porosity measurements of the layers.

At last, Appendix C presents the defects of structures during processing.

2. LITERATURE REVIEW

2.1. BIOMATERIALS

According to Williams, biomaterials can be defined as natural or synthetic substances that intend to interact with biological systems, to substitute partially or totally tissues, organs or functions of the body with the mean of keeping or increase life quality of the patient, without stimulating any adverse biological response to the host. Function and durability within the body vary considerably according to the need of each application and composition of introduced material (WILLIAMS, 2009).

Cardiovascular and orthopedic prosthesis, dental implants and medical devices are some of many examples of applications in different biomedical areas. Products that, besides offering mechanical support functions, also stimulate growth of new tissues and/or have controlled release drug systems, are among central themes of current researches of biomedical engineering, to provide a faster and more efficient healing to the patient (RATNER et al., 2013).

Metals, polymers and ceramics/glass, and all their respective features, can be used within human body. Those are generally classified by its biological response; materials that show no interaction with body, and retain its structure after implantation, are called bioinert; those which promote bonds with living tissue are called bioactive; and those which are degraded and replaced by regenerating natural tissue, are called biodegradable.

Biological responses are directly influenced by the surface of biomaterials and medical devices. Chemical and structural conditions of the surface enable bone growth, improve wear and corrosion resistances, and affect the long-term of implant, among others. Coatings or even changes on original surface might promote an increase in performance and biointeraction of clinic products, without modifying initial design and function, or need of retraining medical staff. Surfaces can be modified by three main processing methods: chemical deposition, coating or physical modification (etching, mechanical roughening) (RATNER et al., 2013).

Implants can mix different compositions in the same product, in order to attend different mechanical request along a body or improve superficial response. The main objective is to reproduce the functions of the natural material that will be replaced. Proper fixation to soft tissues

is important to achieve high resistance to mechanical loadings, and eventually promote tissue-growth.

Osteointegration is the term applied for lamellar bone attachment to implant without intervening in fibrous tissue. It is required to reduce occurrence of stress shielding (from unequal load distribution between implant and bone) that leads to weakening of the host bone (MEHRALI et al., 2013). Bone ingrowth occurs inside a porous surface; it requires pore size range of 50 to 400 μm, and percentage of voids of 30 to 40% to preserve mechanical strength (KHANUJA, 2011). Growth rate is influenced by pores size and interconnectivity of pores; on the other hand, it is not affected by pore shape (RATNER et al., 2013).

Therefore, the presence of porosity is considered an advantage for biomaterials, needed in many applications. In contrast, porosity acts as source of crack propagation, restricting selections of materials and processing conditions (JAMALUDIN et al., 2015).

Ceramic materials are intrinsically linked to porosity. Combined to advanced ceramic properties, it becomes an excellent option to perform as biomaterial, particularly on orthopedic and dentistry fields. Ceramic components are mainly found in total joint arthroplasties (TJA), coatings on implants and devices, and dental restorations (MCENTIRE et al., 2015).

Great part of products used in this class of materials are composed by alumina, hydroxyapatite (HA), glass-ceramics and zirconia; and resorbable compositions include calcium sulfate, tricalcium phosphate and calcium-phosphate salts (RATNER et al., 2013). Hydroxyapatite is a calcium-phosphate ceramic, with similar composition of bone and dentin minerals. Known for being osteoconductive – that induces formation of new bone tissue –, it's the most "famous" bioceramic used on substitution of bone tissues, bone grafts and teeth (OLIVEIRA, 2010). Alumina is the pioneer of ceramic biomaterials for its well-known mechanical properties; it is bioinert and resistant to corrosion at *in vivo* environments. Glass-ceramics have become known as bioactive ceramics, allocated on implant's surface to create an adherent interface that withstands high mechanical stresses (RATNER et al., 2013). And zirconia is the one with best mechanical properties, perfect to load-bearing applications. Its bright color also enables it to be applied on dentistry, adjusting composition to match the teeth color of the patient.

The interest for all-ceramic implants has grown with the development of new processing technologies and with favorable clinical observations. For example, the need of cement in metallic implants to

promote fixation has brought biological problems related to wear debris; this leads to development of all- ceramic cementless implants, with improved design, increased durability and most recommended to young patients, who request higher mechanical loads and longer useful life (PETSATODIS et al., 2010; KHANUJA, 2011). On dentistry, advantages of metal-free implants increase all-ceramic systems demand, by aesthetical improvement and lower biological response (MIYAZAKI et al., 2013).

Thus, the selection of biomaterials and its manufacturing techniques must consider function, interaction expected to host body, and also the environment that it will be applied. All conditions can cause structural changes on material and compromise its efficiency (RATNER et al., 2013).

Dental materials

The progress on aesthetic aspects of artificial teeth has brought loss of mechanical strength due to fragile nature of ceramic materials. Adaptions on compositions turn adversities into suitable properties of dental restorations, withstanding different conditions of humidity, pH, cyclic loadings, among others.

All-ceramic implants conquered dentistry with products of good mechanical properties, resistance to oral environment, competitive price, and good aesthetics, favorable factors for the complete replacement of metals on oral implants. Compositions can vary depending on design of implant, for being necessary different characteristics in each place of the piece. Generally, core structures are made with polycrystalline ceramics with higher strength, such as zirconia and alumina, while superface covering consist of porcelain and/or glass to achieve pleasing aesthetics (KELLY; BENETTI, 2011).

Its combination with metals provides dental implants with excellent properties but unwanted aesthetic effect. So, the last three decades were crucial for dentistry to develop technologies for production of all-ceramic systems, such as hot-pressing, slip-casting and, the most recent, CAD-CAM (Computer Aided Design-Computer Aided Machining) (DENRY; HOLLOWAY, 2010).

Dental implants are generally composed of three main parts, as shown in Figure 2.1: (a) the central structure fixed to the gum tissue, playing the role of tooth root; (b) the core structure, an abutment attached to the fixed structure, associated with pulp and dentin; and (c) the crown, the outer part of the tooth. Thus, each part has the specific

function of replacing certain structure of the tooth. Structure (a) is commonly made of metal for being easier to machine, but there are also options of ceramic models. Structure (b) is generally made of zirconia based ceramics, due to its mechanical resistance. And the last structure (c) is composed by a mix of zirconia and porcelain and/or glass, with function of aesthetic finish and protection of aggressive conditions of mouth.

Figure 2.1 - Structural comparison of a natural tooth and a metal-ceramic implant.

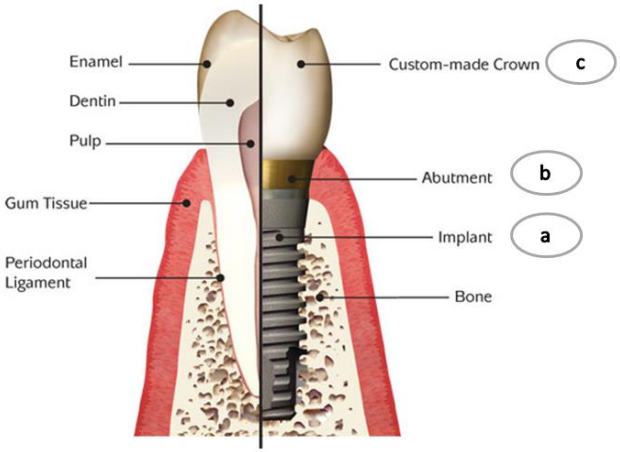

Source: Dental implants, 2017.

Replacement of dental crowns should reproduce structural transition from dentin to enamel. It is important to emphasize that transition between both materials must be sufficiently consolidated to avoid detachment during use (BARANI et al., 2012). A wide range of surface modifications is used in dental implant, from structural changes (mentioned in previous chapter) to adding material (adhesives, sealants, etc.). This process guarantees consolidation of two or more materials (ZHANG; KIM, 2009).

Transition between substructures shall be made with absence of stress zones derived from mismatch on mechanical or thermal properties on contact of different materials. Natural tooth show a distribution of properties along its extension, which can help on support of mechanical stresses. In addition, clinical cases verified that abrupt transition of

structures (b) and (c) could be the reason of early failures on dental implants, by detachment of those two materials (BARANI et al., 2012).

In this way, many techniques are being studied in order to soften this transition by creating a functionally graded material (FGM's), for example, in order to mimetize nature with its capability of stress distribution (ZHANG; KIM, 2009).

Some variables can affect performance, reliability and useful life of implants, including intrinsic and extrinsic factors. Intrinsic factors include amount of crystalline phase, which varies from 35 to 99% vol., size and geometry of crystals, mismatch of Young´s modulus and/or thermal coefficients between core and surface; also processing conditions play a fundamental role on the control of its microstructures. Extrinsic factors are the aggressive environment of mouth, including great variation on pH, temperature, humidity and loads – cyclic and peak loads –, that expose materials to degradation and corrosion on contact with humidity even at low temperatures. Mechanical characterization under humidity and cyclic loading is necessary to attest quality and reliability of products (LAWSON, 1995; KELLY, 1999). Oral adversities can be the major cause of early failure of dental implants (DENRY; HOLLOWAY, 2010).

However, crystallinity is only one of the factors that contribute to material's performance. Crystal's size and geometry, modulus of elasticity, phase transformation and compatibility of thermal expansion coefficients (among dissimilar materials) are also responsible for their performances (DENRY; HOLLOWAY, 2010).

In the quest to minimize defects originated in interfaces within a structure, development of all-ceramic pieces has gained space in the market, with zirconia as the main protagonist, in the YSZ form, playing the role of both implant (1) and abutment (2). But aesthetic finishing recovering are still needed in dental crowns. Therefore, some studies turn their attention to this interface, in an attempt to create ideal conditions for a healthy transition. At this point, concepts of FGM (discussed in chapter 2.4) showed interesting designs to solve this issue.

2.2. ZIRCONIA

Success of zirconia ceramics was due to a combination of strength, toughness and chemical resistance, allowing it to be used in applications on harsh environments and under severe loading conditions. Studied since 1960´s, this material is extensively used as thermal barrier coating (TBC) in gas and jet turbine engines, membranes in solid oxide

fuel cells (SOFC), optical coatings, security devices, knife blades and cutting tools, oxygen sensors, biomedical devices, among others (LUO et al., 1998).

The zirconium oxide, with formula ZrO2, has three possible crystalline arrangements: monoclinic (m) structure at room temperature, tetragonal (t) structure for temperatures from 1170°C to 2370°C and cubic (c) structure for up to 2370°C, with melting point at 2716°C. During cooling, transformation t→m is accompanied by a volumetric expansion of 3 to 5%, which generates stress on microstructure that could lead material to fracture; but it's also the key for toughening mechanisms. The discovery that addition of elements could control structures and/or phase transformations on zirconia based ceramics has sparked the interest in scientific community for its similarity with steel alloys, both exhibiting martensitic transformation at relative low temperatures, used to enhance strength and fracture toughness at controlled compositions. For this reason, zirconia alloys were also known as "ceramic steel" (HANNINK et al., 2000).

So, the use of small amounts of stabilizers has become very common to keep metastability of tetragonal and/or cubic phases (high-temperature phases), at room temperature. Different oxides are used to stabilize partially or totally those phases; generally, alkaline earth oxides, such as CaO and MgO, are used for partially stabilized zirconia (PSZ), while Y2O3 and CeO2 are used for stabilization of t phase, such as tetragonal zirconia polycrystals (TZP), and cubic phase, fully stabilized zirconia (FSZ). These systems are usually named associated with added component (ex.: Mg-PSZ, Y-TZP, etc.) (KELLY; DENRY, 2008).

The toughening mechanism on TZP systems occurs on fine grains of metastable t phase that transform by cooling at temperatures lower than 25°C or is induced by stress, in regions around a hardness indentation or surrounding the tip of a crack (Figure 2.2). Volumetric expansion of the grains blocks crack propagation and prevent forming new cracks. Modifications on microstructure occurs locally on presence of stress, where is visible some m laths between t grains (predominant). In PSZ systems, metastable t phase with lenticular grains are precipitate in a stable c phase matrix. The metastable phase can transform spontaneously in m from rapid cooling of high temperatures, and under a stress field (HANNINK et al., 2000).

Figure 2.2 - Schematic representation toughening mechanism of zirconia, by t→m transformation on a induced crack.

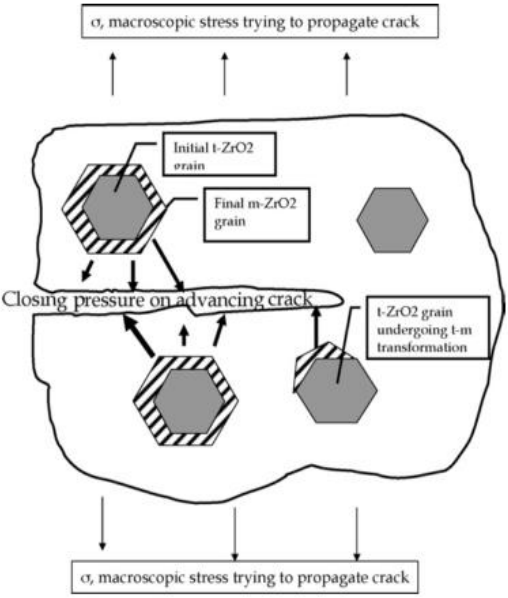

Source: LUGHI; SERGO, 2010.

This mechanism has become so well known that use of zirconia based ceramics has been easily diffused in medical and dental areas by its efficient mechanical performance, replacing metal alloys on many devices. In 2001, a setback has slowed the production of zirconia medical products due to failures of 400 implanted devices in a short period, occurred by aging of the microstructure in contact with body fluids. This episode was due to a change on the process parameter on a factory of zirconia prostheses. At that time, thousands of zirconia prostheses had already been implanted around the world, especially in the USA and Europe, which have brought concerns about standardization of implant materials. This episode has put zirconia momentarily in check for "inside-body" applications, until studies disrupted functioning and effects of aging mechanisms (CHEVALIER, 2006).

This phenomenon, also called low thermal degradation (LTD), is defined by the spontaneous t→m transformation at low temperatures, without influence of any local load. The contact with water induces transformation of t grains, which expansion provokes uplift on the

surface and pushes the untransformed grains around, creating a stress field (Figure 2.3-b). But micro cracks may appear from displacement of m grains, facilitating the entry of water into the structure, and thus, increasing amount of m grains that tend to peel off from structure (Figure 2.3-c). The effects of aging include loss of mechanical properties, density and toughness, accompanied by macro and micro cracks and increased m phase content. The intrinsic factors that influence LTD's susceptibility are: type and amount of stabilizer, grain size and residual stresses (LUGHI; SERGO, 2010; PICONI, C., 2011).

Figure 2.3 - Schematic representation of partially t→m transformation of zirconia grains, and how tensile stress is introduced into the microstructure on LTD phenomenon.

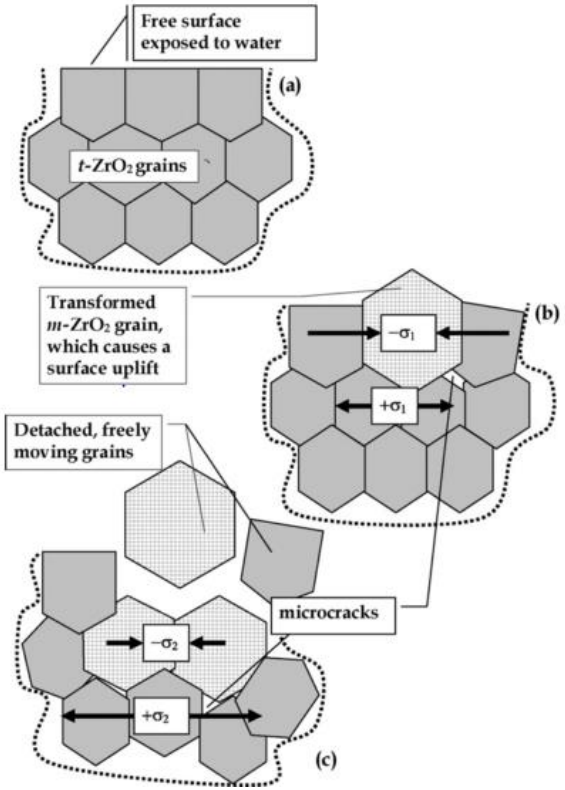

Source: LUGHI; SERGO, 2010.

Despite all efforts to prevent this phenomenon, zirconia cannot be considered an aging-free material since transformation is a natural tendency to monoclinic equilibrium state. But kinetic of transformations are strongly influenced by microstructure, which, in turn, is affected by small amounts of additives.

Yttria stabilized zirconia

Addition of yttria to zirconia causes microstructural changes that allow its performance in different fields due to its chemical inertness, thermal stability and high ionic conductivity at high temperatures. Depending on added amount, phase diagram varies temperature of m, t and c phases transformations, as seen at its phase diagram in Figure 2.4; and consequently varies its main characteristics by its microstructure.

Zirconia ceramic with 8% mol. yttria is among most used commercial zirconia "alloys". It is considered a FSZ for its predominant cubic phase structure, with increased stability at high temperatures. Any composition with cubic phase at beginning of firing, and intact structure at room temperature, can be considered "fully stabilized". Cubic zirconia has a very low thermal conductivity, desired property for thermal coating barriers (TBC); also shows high ionic conductivity for oxygen at high temperatures, used as fuel cell membranes (MARTIN, 2011).

The substitution of Z^{4+} for Y^{3+}, on charge stabilization of yttria-zirconia mixture, creates oxygen vacancies that act on stabilization of tetragonal and cubic phases, but also increase ion conductivity. Addition between 4 and 10% mol. of yttria results in a favorable proportion for ion conductivity.

The TZP has predominant tetragonal phase in its structure, stabilized with 2 – 4% mol. of yttria, with small crystal grains associated with improved strength, fracture toughness and resistance to wear and aging. It's prone to toughening mechanism that increases its fracture resistance, able to be applied as a structural material. It has been seen in industrial parts and everyday products, such as ceramic knives (KELLY; DENRY, 2008), but it is on biomedical field that has been gaining more space. Medical applications of Y-TZP include surgical tools, instrumentation, surgical implants, orthopedic (femoral ball-heads), while dental applications include full and partial coverage crowns, orthodontic brackets, implant abutments, veneers, extracoronal attachments, among others (VAGKOPOULOU et al., 2009).

Figure 2.4 - Portion of the phase diagram of ZrO2 – Y2O3 system.

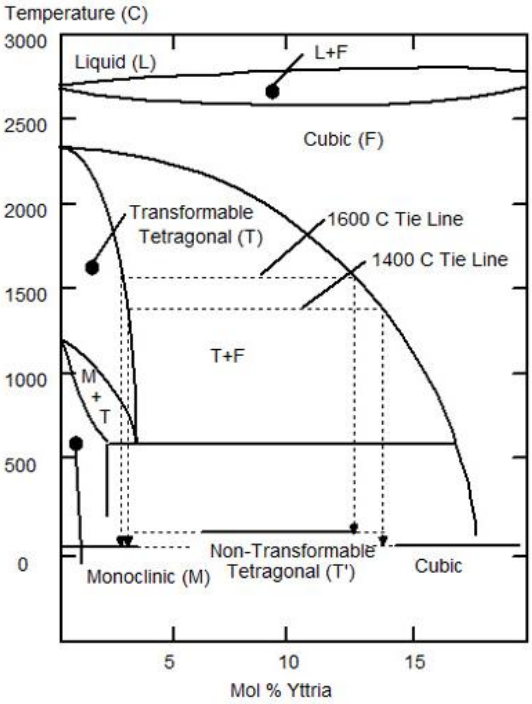

Source: AZO, 2017.

Commercial zirconia is often produced with binders and other additives that facilitate its processing, and guarantee non-incidence of aging. Its good mechanical characteristics combined with toughening mechanism and biocompatibility, have made it the main competitor of titanium, used in biomedical load-bearing applications, and overcome properties of alumina, as shown in (Table 2.1).

Table 2.1 - Mechanical properties of Y-TZP, titanium and alumina.

Properties	**Titanium**	**Y-TZP**	**Alumina**
Density (g/cm³)	4.51	6.00	3.97
Elastic Modulus (GPa)	110	206	300
Compressive strength (MPa)	240 – 550*	800 – 1300	2100
Hardness (kg/mm²)	23	1000 – 1400	1000
Fracture toughness (MPa.m$^{1/2}$)	70	6 – 15	3.5

***** Tensile strength (Source: PCI; Tosoh Co.)

2.3. POROUS STRUCTURES/POROUS CERAMICS

Porous structures have already been considered problematic from a mechanical point of view, with limited applications. Over time, porosity has become known to be associated with thermal insulation, acoustic properties, permeability and increased surface area, brought the interest of new fields of applications and development of porous materials (COLOMBO; SCHEFFER, 2005).

All classes of materials have examples of porous structures; cellular properties of both are influenced by the same set of factors, which include: (i) mechanical properties of (dense) material; (ii) amount and morphology (shape and size) of pores; (iii) connectivity of pores; and (iv) relative density. These factors will dictate the mechanical, electrical and thermal properties of the final piece (COLOMBO; SCHEFFER, 2005).

According to IUPAC, porous structures are classified by the average pore size range: *microporous* to < 2 nm; *mesoporous* 2 to 50 nm; and above 50 nm, macroporous (PERKO, 2012). Interconnected pores, also known as *open porosity*, composes fluid (liquid or gas) transport structures, like scaffolds and others biomedical applications, filters and catalyst supports; while pores that are not connected with others, called *closed porosity*, are very common on thermal insulators, such as refractories, kiln furnitures and heat exchangers. Thus, interconnectivity of pores influences thermal properties of materials (WERR, 2014).

The combination of porous structures and ceramic materials results in low density, high stiffness and low specific heat bodies. These

characteristics are essential to technological applications like filters for molten metals and hot gases, and biomedical devices. A variety in shape and distribution of pore form several structures such ceramic foams, honeycombs and hollow spheres (COLOMBO; SCHEFFER, 2005).

Among many processing routes to obtain porous ceramics, there are: the use of sacrificial templates, use of narrow particle size distribution and controlled sintering stage. Sacrificial templates are widely used for porous solids fabrication, using incorporated components in the ceramic matrix to produce the pore structure, through its removal by thermal treatment. It is also very common the use of gas as pore former agent, introduced into ceramic suspension/slurry and removed after solidification of the body; its morphology determines size and shape of pores. Generally, formation of pores by this method occurs through formation of foams, consolidated by sintering, requiring additives as surfactants, turning it to complex systems (STUDART et al., 2006; WERR, 2014).

Sintering considers work with different temperatures to reach a proper diffusion rate. Ceramics generally follow a specific densification curve; first, the increase of temperature induces volumetric diffusion, that creates necks among particles, called as pre-sintering stage; and after that, higher temperatures lead to higher diffusion rates, increasing densification and shrinkage of material. Depending on diffusion, it can control porous systems (WERR, 2014).

Through the control of particle size distribution of ceramic powder, it's possible to predict its packing density. For example, unimodal distributions of spherical particles, with narrow range of sizes, have lower density in its packing arrangement. The space between spheres is large enough to not collapse during sintering (

Figure 2.5), forming pores with controlled size by controlling heat treatment steps (WERR, 2014).

In this mechanism, a previous consolidation on ceramic powder surface may be necessary in order to prevent closed porosity during sintering of the body.

Porous films manufacturing techniques are being developed to enable surface modifications of technological products. These modifications are important to increase superficial areas, create interfaces, and stimulate external responses in contact with another material and/or tissue. *Dip coating*, *slip* and *tape casting* are methods that use ceramic suspensions on formation of porous membranes, with controlled range of porosity and thickness. Other techniques are used to

promote partial densification, pore orientation and heterogeneous distributions of voids along a section.

Figure 2.5 - Schematic difference on packing of two particle size distributions.

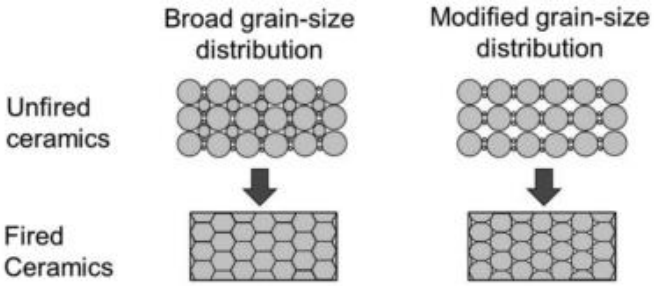

Source: WERR, 2014.

2.4. FGM

Functionally graded materials (FGM) combine two or more dissimilar materials by a gradient transition of structure, composition and/or morphology along a section, resulting materials with adequate properties distributed along a body, to attend different mechanical needs. A soft transition helps to improve adherence and decrease mismatch of mechanical, thermal and even chemical properties (MEHRALI et al., 2013).

Incorporation of two, or more, component's function in the same body is the main objective of this class of materials, using artifices as variation of composition, porosity, geometry and physical state as a manner to obtain the mixture of functions (MIYAMOTO et al., 1999). The transition may occur continuously or discretely, in layers format (

Figure 2.6). The first one is widely observed in nature, while the second, in laboratories. Replications are not always an easy task, and creation of artifices is often necessary to achieve the goal. The difficulty to reproduce continuous transition attracted attention to layer deposition techniques, as dip coating, tape casting, chemical vapor deposition (CVD), among many others, to recreate structures discretely. Dense layers between porous ones are still characteristic of FGM (UDUPA et al., 2014).

A great number of nature structures with some gradation of property along the body served as example to create and develop this

material concept. Among them are the bamboo, shells, teeth and bones (Figure 2.7) all of them with gradual structures according to environmental conditions and mechanical request (MIYAMOTO et al., 1999).

Figure 2.6 - Schematic illustration of FGM transitions: (a) continuous, and (b) discrete – by layers.

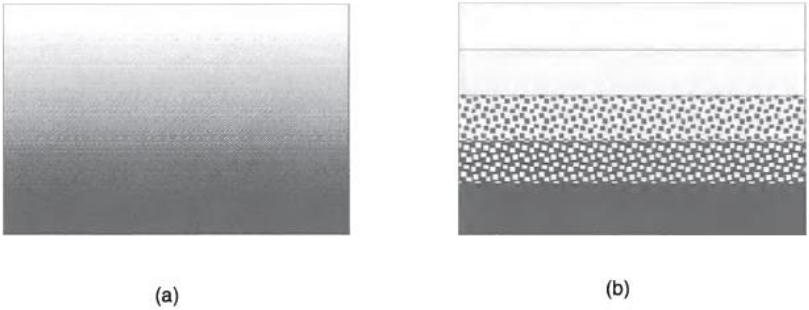

Source: MIYAMOTO et al., 1999.

Figure 2.7 - Examples of nature's FGM microstructures: (a) bamboo, (b) mollusc, shell, and (c) tooth enamel.

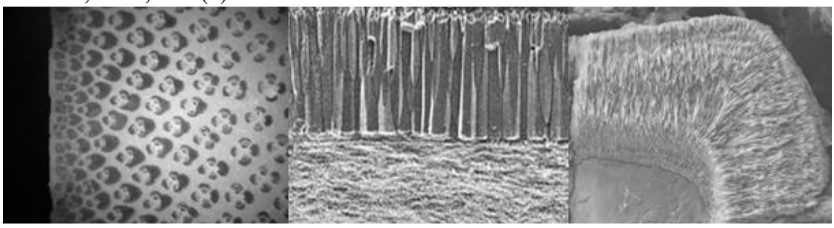

Sources: Adapted from MIYAMOTO et al., 1999.

The increasing interest on biomaterials with functional gradient allows the advancement and applicability in different biological branches: photosynthesis, self-cleaning and self-healing materials, controlled-release drug systems, implants, among many others. Soft transitions are often found in surface areas by coatings; this concept enables surface modifications of medical devices and implants, improving its interaction with body fluid, acting as chemical shield, increasing surface area, or even for aesthetic finishes. An option to promote those characteristics is by surface porosity; a way to reproduce nature and improve efficiency of existing products is by creating a

gradient of porosity, which improves structural conditions of material to serve as an interface with another (MARTIN, 2011).

Gradient porosity

In the human body, several structures with heterogeneous distributions of pores are seen, as the case of bones which surface is denser than its nucleus undergoing a gradual porosity transition (Figure 2.8). That configuration, also called sandwich structures, leads to an increased bending resistance when compared to a solid beam. Porosity gradient on biomaterials are also attractive to improve interaction between dentin and enamel, on dentistry (MEHRALI et al., 2013). Interconnectivity of pores may act as an organizer of vascular channels, ensuring supply of blood and nutrients to the bone (MIAO; SUN, 2009).

Heterogeneity of porosity (size and amount), composition and mechanical properties may result in structural, biological and mechanical optimization of porous biomaterials. The gradient of pores can further induce "guided" growth of new tissues and cells (MIAO; SUN, 2009). This configuration also reduces residual thermal stresses on contact between dissimilar materials, leading to early fracture of products (MANICONE et al., 2007).

Figure 2.8 - Internal gradient porosity configuration of a human bone.

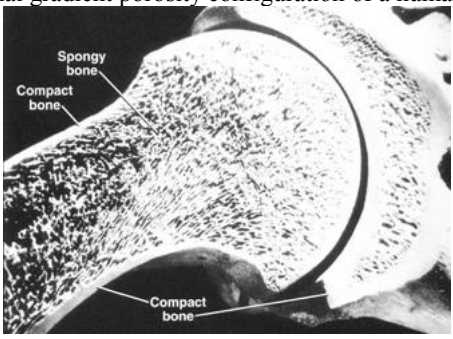

Source: University of Cambridge, 2017.

Examples of basic shapes that vary porosity content along a section can be seen in Figure 2.9. This structure configures a specific arrangement of the so-called functionally graded materials (FGM's), because it changes its properties over a zone.

Figure 2.9 - Possible configurations of porosity gradient: (a) block, (b) block with dense layer, (c) disk with dense layer, and (d) cylinder with dense core.

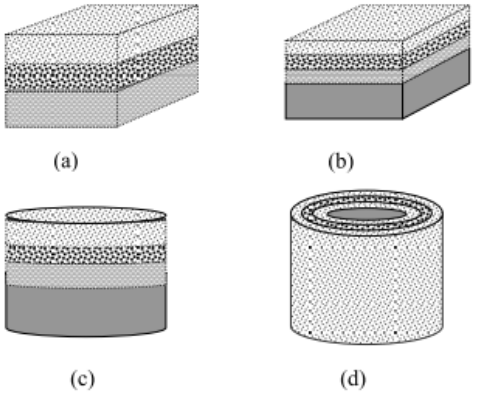

Source: Miao & Sun, 2009.

As mentioned at the beginning of the chapter, the gradient can be made continuously or by discrete configurations. Continuous transitions techniques are usually more expensive and require complex equipments, such as freeze-casting, spark plasma sintering (SPS) and electrospraying (into a template); while others, which result in discreet layered gradient, are usually cheaper but may take longer to be produced, due to the need for multiple depositions. Techniques for discrete porous gradient structures are: sintering of graded particles, multiple tape casting or dip coating, and slip casting. Figure 2.10 represents consecutives depositions of layers, with distinct pore sizes, forming a graded structure (MIAO; SUN, 2009).

To produce porosity in layer deposition methods, there are two main routes: introduction of pore formers, such as polymers or foams, to be eliminated by firing at relative low temperatures and controlled heating rates (in order to avoid cracks generated from the extraction of the component); or by particle size control, so that porosity comes from interparticle voids formed during its packing, as discussed in chapter 2.3.

Figure 2.10 - Illustration of deposited porous layers with gradient pore sizes.

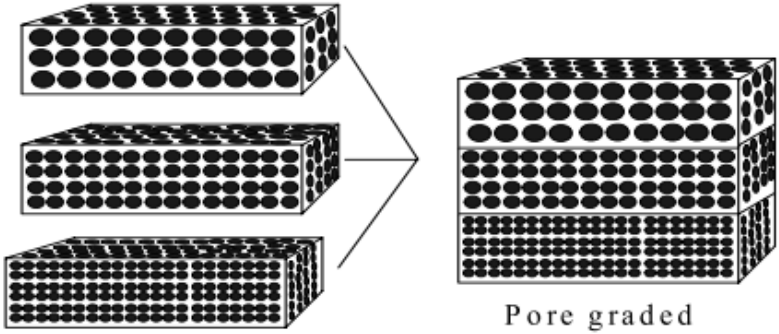

Source: Miao & Sun, 2009.

2.5. DIP COATING

Dip coating is a deposition process that uses simple mechanism of attraction to retain particles on a given substrate – cappilarity. The technique basically consists of immerging vertically a porous substrate in a suspension containing precursor powder, to form a film of particles adhered on substrate's surface via capillary pressure (BRINKER, 2013). The process can be divided into four main stages: (1) immersion and dwell time, (2) deposition, (3) drainage and (4) evaporation.

Figure 2.11 - Schematic illustration of dip coating process, and its steps.

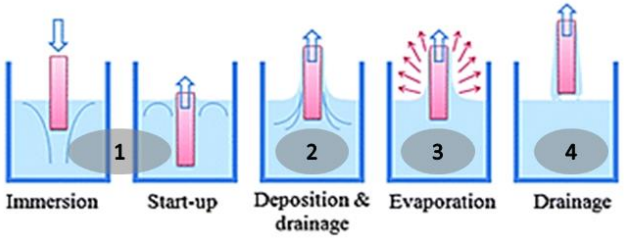

Source: Royal Society of Chemistry, 2017.

The thickness is controlled according to process parameters, such as speed of withdraw, temperature and atmosphere; and chemical, such as dilution and solvent. A certain dwell time is necessary to guarantee complete wetting of the substrate during coating, which may difficult by high surface tension of solvents (GROSSO, 2011).

Deposition stage depends on suspensions characteristics, such as solid content, particle size, additives, and on substrate's structure, such as porosity and pore size. During withdrawal of the substrate, the upward movement drags the penetrated liquid into pores, while outer part returns to the bath, draining excess liquid from the surface (Figure 2.12-A). Evaporation phase completes film deposition cycle, while a subsequent heat treatment is often necessary to eliminate organic residues and/or promote crystallization of functional oxides (BRINKER, 2013).

This method showed to be very attractive due to its simplicity, easiness access, regular control of thickness, waste-free, and low energy associated. Its drawbacks are basically related to drying, when excessive retraction of thick layers may provoke cracks.

Withdraw speed influences on thickness by two different regimes: draining, on high speeds (> 10 mm.s-1); and capillary, under ultra-low speed (< 0,1 mm.s-1). This trend is represented by graph below (Figure 2.12-B) where thickness increases on both extremes of graphs, with an intermixed regime between 0.1 and 10 mm.s-1, ideal for thin layers fabrication. The dilution of the medium causes a downward shift of the curve.

Equation 1 (Figure 2.12-C) represents the sum of both regimes resulting the curve (B) below; capillary term can be described as the evaporation rate divided by speed (E/u) –, and draining regime, solution characteristics times speed ($Du^{2/3}$). So, thickness is dependent on a solution composition constant k_i, withdraw speed u, evaporation rate E, substrate width L, and physical-chemical characteristics of solutions D. Both regimes are counterbalanced by evaporation (GROSSO, 2011).

Figure 2.12 - (A) Driving forces acting on deposition; (B) thickness versus withdraw speed and the three regimes of deposition; and (C) thickness equation, considering dependence of deposition regimes.

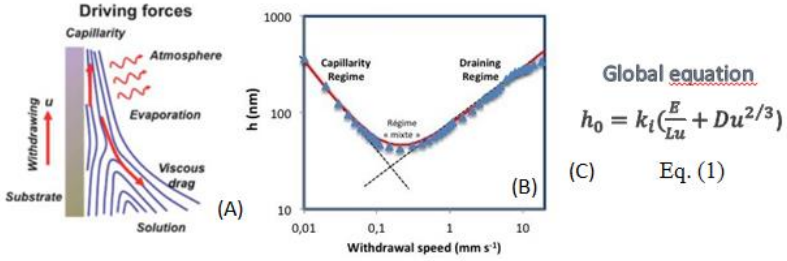

Source: Adapted from (GROSSO, 2011).

Capillary pressure on porous substrate is responsible for particles to concentrate at the substrate-suspension interface and, thus, forms a film, since particles cannot “penetrate” further in the solid. It represents a very strong driving force to densify depositing film, and can be estimated by mathematical approaches.

The medium containing precursor material, may be in the aqueous form, emulsion form or, the most applied of them, in sol-gel form. That is because sol-gel, and other chemical solution depositions (CSD), in some cases, increase wettability of substrates and improve film formation ability (KOZUKA et al., 2012). Nowadays, a wide range of technological applications uses sol-gel processes on coatings, such as sensor and actuators, superconducting layers, protective coatings, passivation layers, among others; therefore, many studies have already disrupted sol-gel mechanisms (BRINKER, 2013). However, other systems do not have the need for additives to improve processes conditions; for these, aqueous based processes can be a simpler and cheaper choice.

Structural control of deposited layers depends on factors related to suspensions (or emulsions, sol-gel, etc.) and process parameters, along with precursor material characteristics. Among them are: solid content and viscosity of suspension, speed and time of immersion, and properties of powder. Particle size has an important role on thickness control. The range of thickness obtained by dip coating varies in 100 nm to 100 μm, just as pores size, depending on precursor powder and processing conditions.

Mathematical and/or computational models are very effective tools for prediction and control of dimensional and structural parameters of formed membranes, although there are some restrictions about tubular shapes, since it involves complex mathematics about radial flows (GU; MENG, 1999).

The dip coating has been applied in dentistry since 1990’s, to infiltrate vitreous material on a ceramic infrastructure (pre-sintered), creating a two-component structurally interconnected material (DENRY; HOLLOWAY, 2010). This type of structure, as mentioned before, avoids defects related to residual stress of different thermal properties contact; it can also enhance restoration’s ability to withstand mechanical loads.

The use of ceramic precursors allows deposition of porous and dense films by this method. The interest in ceramic membranes reaches several areas: electrical, electronics, biomaterials and energetic are a few. YSZ plays a key role in applications such electrolyte films for solid

fuel cells (SOFC) and filtration membranes, and also on orthopedic implants, due to their good biocompatibility and bone ingrowth property (LENORMAND et al., 2005; MIAO et al., 2007).

The processing in industries is normally made with special equipment to control process parameters, such as speed and immersion time. In this way, process conditions are standardized, with controlled thickness and layer structure.

It is very common the use of additives to form pore structures, by foam production and subsequent pyrolysis to exterminate residue materials. Techniques with aqueous suspension dismiss the need of a great number of those additives, but dispersant is an essential component of ceramic slurries. It prevents agglomeration of particles, ensuring homogenization of the system; and also affects viscosity, generally very important to determine process parameters.

Particles packaging factors/mechanisms

Packing arrangement of particles plays a decisive role in controlling porous systems. It is affected by few factors, such as:

- Particle size distribution;
- Particle's morphology;
- Particle's density;
- State of dispersion;
- Processing of conformation.

Monodispersion arrangements, which considers a unique size of spherical particles, such as atomic structures for example, predicts packing factors of 0,60 and 0,64, reaching up to 0,74 in ordered structures (CFC). Spherical particles, besides possible to predict its behavior, reach higher packaging densities when compared to non-spherical, as shown in Figure 2.13 due to friction during conformation that produce voids among particles. Therefore, grading curve and particles morphology have effect on densities arrangements.

Figure 2.13 - Relative packing density as a function of particle's morphology and size.

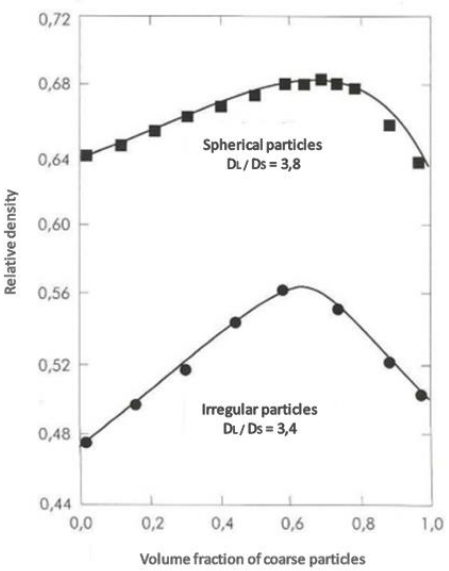

Source: OLIVEIRA, 2000.

Monodispersions are considered discrete distributions of particles with a single size in the system; a rare situation at industrial field. Unimodal distributions exhibit a unique average size of particles; bimodal, two different average sizes; and multimodal, more than three peaks of average sizes. Those curves can be narrower or wider, or even present discontinuities, such as small gaps with absence of a certain particle size.

Figure 2.13 shows the packing density of bimodal distributions of spherical and non-spherical particles. The peak of maximum density of both curves is reached by similar volume fraction of coarse powders, not depending on its format. However, bimodal distributions may exhibit different particle shapes; the higher amount of non-spherical particles, in relation to a mixture containing both types, the greater tendency to produce porosity, as shown in Figure 2.14.

Figure 2.14 - Porosity of a mixture as a function of relation between angular and spherical particles.

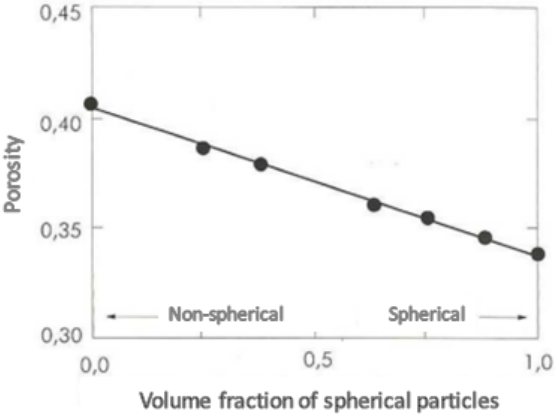

Source: OLIVEIRA, 2000.

Internal porosity of particles also implies a lower packing density, since they can show close pores (like hollow) or open pores (like clusters). Sharp difference in particle's densities of bimodal distributions can generate heterogeneous density in a product during its conformation, compromising mechanical performance and/or reliability. Sharp difference on pore sizes of a system may lead to the "wall effect", that happens when fine particles interact with coarser ones as if they were almost plane, like a wall. This phenomenon is even greater when the coarser powders present porosity, attracting them by capillarity (Figure 2.15).

Figure 2.15 - Illustration representation of low density packing due to "wall-effect".

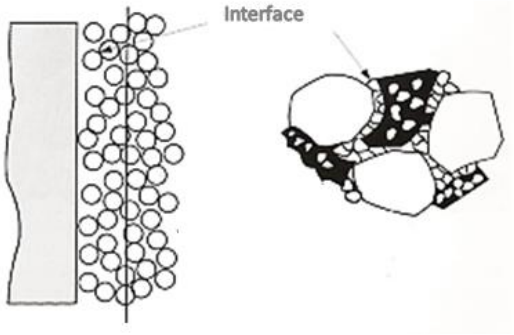

Source: Adapted from OLIVEIRA, 2000.

The manufacturing method can use dry and wet routes. The difference between them is presence of water, associated with greater mobility of particles. Dry routes, as pressing, can increase low packing levels; while wet routes, which includes suspensions, are often subjected to capillary forces while depositing on a face (dip coating, slip casting, etc.). Each of these methods has certain influence on particle's compaction, with the last one showing lower (and random) packing levels. When fluid media are part of the process, the state of dispersion must be considered to maximize packaging (CASTRO; PANDOLFELLI, 2009).

Due to many factors that contribute to packaging, mathematical models has described density behavior of mixtures using different size distributions of powders. There are two basic concepts: Furnas model, which its individual particles approach; and Andreasen's model, with its continuous distributions approach. Further studies concluded that both concepts express the same idea, by different visions; so, a mathematical convergence brought together both concepts into a single equation, known as Alfred's model (eq. 2).

$$CPFT\ (\%) = 100\left(\frac{D^q - D_S^q}{D_L^q - D_S^q}\right) \qquad \text{Eq. (2)}$$

where CPTF is the "cumulative percentage finer than" D – particle diameter; DL is the diameter of largest particle and DS, the smallest; and q is the distribution's coefficient. Computational simulations have

verified that values of q lower than 0,37 might promote maximum packing, while higher values leads to a residual porosity. The distribution coefficient is affected by amount of fine particles; the greater the quantity of fine particles, the smaller the value of q.

However, increase fine particles (~1 μm) fraction may interfere on size distribution. The tendency to agglomeration is by increase of relation between surface area and volume, for small particles, that increases interparticular cohesive forces. Its presence tends to inhibit spatial coordination of higher packing densities, thus, increases void volume (CASTRO; PANDOLFELLI, 2009).

2.6. CURRENT TECHNIQUES

Along this section, several production techniques of homogeneous and graded porous structures have been introduced. A comparison of currently used techniques is presented (**Erro! Fonte de referência não encontrada.**), relating porosity, pore size obtained in each referenced work, and the need of pore-forming agents, which increases time of production due to its removal.

The references that made porous structures by the dip coating method (first lines) used raw materials with particle sizes below 5 μm. With zirconia, the largest pore size was 60 μm produced with particles of unspecified size, while alumina, the maximum was 190 μm, both with high porosity (%).

Methods such slip casting and gel casting are mainly used for porous solids production, that is, solids with similar dimensions (not as a layer). Tape casting, widely used in the production of layers, was seen only in cases of average pore size of 2.5μm. The tape casting and gel casting papers have studied production of porosity by addition of pore former agents.

Powder metallurgy is cited for being related to mechanisms of spherical particles packing, in this case, using particles of great granulometry (> 180 μm) to form structures with varied pore sizes (gradual transition). The main difference between this and the present work, lies in the physical properties of the raw materials (metal vs. ceramic) and its behavior during sintering.

Vacuum casting was used to obtain large pore sizes, between 300 and 500 μm, burning expanded polystyrene for its formation. Eletrophoretic deposition (EPD) and electrohydrodynamic spraying (EDS) are methods based on the addition of sacrificial materials, and are

attractive for allowing production of varied pore sizes. On the other hand, this information was extracted from reviews from both methods, and its possibilities of applications; for this reason, many processing details have been omitted in these documents. The full articles are not available on free research platforms.

The present panorama highlights a lack on studies of zirconia macroporous structures processing. In this context, the present work intends to insert an inexpensive and simple alternative to obtain surface macroporous structures.

Method	Material	d_{50} (μm)	Pore former	Porosity	Pore size (μm)	Application	Author(s)
Dip coating	Zirconia	5.0	Particles packing	58%	0.9-15.5	Filtration membrane	Maia, D.F. (2006)
	Zirconia	0.15 and 0.80	Particles packing	30 and 42%	< 2.0	Fibre-matrix interface	Blaese, D. (2013)
	Zirconia	*	Decahydronaphthalene (EDH) oil (emulsion)	< 83.7%	60	Thermal insulation	Santos, D.S.F. (2015)
	Zirconia-Titania	< 0.1	Particles packing	11-25%	0.1-0.4	Electrodes for air monitoring	Silva, S.A. (2015)
	Alumina	0.6	Sucrose	70%	190	Biomaterials	Camilo, C.C. (2010)
Slip casting	3Y-TZP	10 – 80	Core-shell particles (nano)	30%	Nano	Dental materials	Perko, S. (2012)
	Alumina APC	0.3 – 95.0	Particles packing	Varied/ Graded	0.1-0.7	Porous gradient solids	Matias, E.M. (2007)
Tape casting	3Y-TZP	0.15	Starch (50 μm)	31.4%	0.15-10	Biomaterials	Albano, Garrido (2012)
Gel casting	3Y-TZP	0.6	Polyethylene (PE) (125-300 μm)	40-50%	2.5	No specifications	Tulliani et al (2011)

Powder metallurgy sintering	Titanium	180 - 1000	Particles packing	35-60%	Graded	Biomaterials/FGMs	Thieme et al (2001)
Vacuum casting	3Y-TZP	0.26	Expanded polystyrene (EPS) (1,40 – 2,95 µm)	51 - 69%	300 – 500	Porous solids/FGMs	Miao et al (2007)
Eletrophoretic Deposition (EPD)	Alumina	*	Paraffin oil (emulsion)	*	*	No specifications	Neirinck et al (2009)[1]
Electrohydrodynamic spraying (EDS)	Zirconia	0.5	Polyurethane (PU) template	Varied	10 - 500	Biomaterials	Muthutantri et al (2008)

[1] Extracted from the review (BOCCACCINI et al., 2010).
* not informed.

3. Optimized route for the production of zirconia structures with controlled surface porosity for biomedical applications

3.1. INTRODUCTION

Ceramic materials based on yttria stabilized zirconia (Y-TZP) present excellent mechanical properties, and are increasingly used in biomedical field due to their biocompatibility. High values of strength and fracture toughness characterize its use in orthopedic prostheses and dental implants, especially as core structures to withstand the higher in-service mechanical stresses (KELLY; DENRY, 2008).

Toughening mechanism of zirconia, involving martensitic phase transformations, allows the material to suppress propagation of cracks, attractive for many technological and "inside-body" applications that require a good mechanical reliability and high resistance at different environments. The mechanism is activated under stress, for example at the tip of a crack, that induces transformation of tetragonal phase (metastable) to monoclinic (stable at room temperature), accompanied by a volumetric expansion of the grains enabling closure of the crack (HANNINK et al., 2000; VAGKOPOULOU et al., 2009).

Biomaterials often require the presence of porosity, either in the bulk or at the surface of a body. Studies have shown the increasing demand for cement-free implants, which improves bone integration by the presence of a rough surface that induces bone growth in contact with the natural tissue (PARK; LAKES, 2007). The porosity is also recommended in prostheses, to a better distribution of stresses to the adjoining bone, thus minimizing the overload episodes and avoiding stress-shielding resultant from significant elastic differences between the prosthesis and bone (HEDIA; MAHMOUD, 2004). Different arrangements of porosity, pore size and its interconnectivity enable the development of various biomimetic structures (MIAO; SUN, 2009).

The layer-by-layer deposition process can be used to elaborate structures with different thicknesses and features throughout a transversal section. The production of multi-layered parts may result, for instance, in functionally graded materials (FGM), known to attach different features in a single part (MEHRALI et al., 2013). In the case of biomaterials, the production of FGMs with porosity gradients is one of the current research targets that tend to mimic natural bones structures, thus combining a porous core with a denser surface (MIAO; SUN, 2009; MUTHUTANTRI, 2009).

Among the available routes used in the production of ceramic layers, the dip coating process has the advantage of being an efficient, simple and inexpensive method (GROSSO, 2011). The process consists in immerging the substrate to coat (porous or dense) into a ceramic suspension and then withdrawn from it after a certain immersion time. The capillary pressure is then regarded for the formation of a wet ceramic coating over the surface with controlled thickness. The possibility of working with any geometry, with basically no material restrictions (as long as in powder format) without unnecessary complications, turns the process attractive to be used in different areas of applications (XIA et al., 2000; KOZUKA et al., 2012).

Despite similarities with other techniques, few are the studies on the formation of macroporous layers using the dip coating method. The use of spherical ceramic particles to produce porosity by the interstices of its packing arrangement is a simple and easy method that required no pore former addition. Therefore, there is no need to eliminate organic additives during the process (MIAO; SUN, 2009).

In this context, the aim of this work is to investigate the adequate processing conditions necessary for the production of macroporous zirconia coatings over zirconia substructures, using the dip coating method and without the presence of pore forming additives.

3.2. MATERIALS AND METHODS

Ceramic powder

In this study, all experiments used 3% mol yttria-stabilized zirconia spray-dried powder (TZ-3YBE, TOSOH Co., Tokyo, Japan) with defined spherical shape. Powder properties are presented in Table 3.1. In order to work with narrower size distribution range, such material was sieved, obtaining particles with average size (d_{50}) of 40 μm and hereafter refereed as Z40 in the text. The powder size distribution was obtained using a particle size analyzer Mastersizer 2000 (Malvern Instruments, Marvern, UK).

Table 3.1- Properties of commercial zirconia powder.

Properties	TZ-3YBE
Granule size $D_{(50)}$ (μm)	60
Particle size $D_{(50)}$ (μm)	0.6
Bulk density (g/cm³)	1.1
Bending strength (MPa)	1000
Fracture toughness (MPa.$m^{0,5}$)	5.0
Hardness (HV10)	1250

(Source: Tosoh Co.)

The first experiments aimed at testing different conditions of the precursor powder on the layer deposited by dip coating. For this, powders were divided into three groups according to the thermal treatment undergone: NT – no treatment; PS – pre-sintering at 1150°C/1h; and S – sintering at 1500°C/2h. Such treatments were made in conventional furnace with no controlled atmosphere. Apparent densities of powders (on different conditions) were experimentally obtained by vibrating particles in a graduated cylinder and, after "laying" of particles, it was noted the respective volume and weight – to apply to the equation: $\rho_{ap} = m/V$.

The addition of fine zirconia particles (d_{50}= 3 μm) to the ceramic suspensions, aiming at increasing the bond strength between Z40 particles, was also investigated as will be shown later. Several fine particles contents (5, 10, 15 and 20vol%) were added to the solid contents of the zirconia suspensions. Those particles, termed "Z3" from now on, were produced by the ultrasonication of commercial zirconia powder suspension (20 vol% of solids in aqueous medium), using an ultrasonic device (Vibra-cell VCX750, Sonics & Materials Inc., U.S.A.). No heat treatment was applied to this material.

Ceramic suspensions

All suspensions were prepared with fixed 30vol% of solid content, and dispersed in water. Previous experiments indicated the need of using different suspending agents in suspensions containing different

powders. Therefore, Darvan C-N (Vanderblit Minerals, LLC, U.S.A.) was used to disperse suspensions with NT powder; while CMC (*carboxymthyl cellulose*, Emfal, Betim, Brazil) was used to suspend PS and S powders. The optimized concentration was 1% and 2%, respectively, in relation to total mass of solids. The mixtures were made by magnetic stirring.

Rheological tests were performed using a viscometer (Thermo Haake VT550 Viscotester - SV 2P sensor, Thermo Fisher Scientific Inc., Germany), at room temperature, varying the shear rate up to 100 s-1, which is the range of the dip coating process (MORENO, 2005).

Dip coating

The dip coating was made on commercial yttria-stabilized zirconia substrates, pressed disks (190 MPa) with 10 mm of diameter – without heat treatment. The depositions were made in Dip Coater equipment (Construmaq, São Carlos, Brazil), using fixed speed and immersion time in 4 mm.s-1 and 5 s, respectively. After deposition, the pieces undergone air-drying (Appendix A) and were then sintered at 1500°C/2h in air atmosphere.

Layers were first coated using suspensions containing powders under different conditions (NT, PS and S), and thereafter, with the best of the three conditions, the test was continued with addition of fine particles. Figure 3.1 systematizes the steps conducted in this study for the definition of the appropriate processing route that leads to the production of zirconia structures with surficial macroporosity obtained by the dip coating method.

Wear test

A simple rotational wear test was applied to evaluate the integrity of the zirconia dip coated layers. The specimens containing dip coated layers made of Z40 powders and fine particles (Z3) were first weighed and then ball milled for 30 minutes in a plastic jar containing 10 alumina balls. The mass loss of each specimen (substrate + coating) was registered in the end of the test.

Apparent porosity and mechanical strength measurements

The difficulty in measuring properties such as porosity and mechanical strength of surficial layers led us to try to reproduce the

porous structures obtained by the dip coating method, but in larger dimension, thus forming porous solids – easier to measurements. Slip casting can be considered similar to the dip coating method for sharing the same main mechanism of material deposition – cappilarity (related to mold/substrate's porosity). In this way, porous solids samples were produced from the same suspensions used in the formation of layers, poured on a cylindrical mold (13 mm of diameter and 30 mm height), with an absorbent base attached (draining water by a single face, without pressuring). The samples dried in stove for 48 h, polished (to ensure parallelism among faces), and then, sintered at 1500°C/2h.

The apparent porosity was measured by ASTM C20-00, weighing each specimen under three conditions: D – dry; I – immersed in water; and W – wet (saturated with water, removed drops from the surface). The apparent porosity (%) expresses the volumetric relation of open pores to external volume. Apparent density (g/cm³) represents the quotient of the dry weight divided by the total volume, including pores. All calculations consider water density as 1 g/cm³, and sintered zirconia (theoretical) as 6,05 g/cm³.

Uniaxial compression tests were applied to these samples. The height disparity of the specimens remained h/D relation between 0,3 and 1,5, as ASTM C133-97 (for uniaxial compressive tests) states. Structures were analyzed via SEM as regard to their morphology, porosity and connectivity of pores.

Figure 3.1 – Flow diagram summarizing the steps involved in the determination of the processing route for the production of zirconia structures with surficial macroporosity by the dip coating technique.

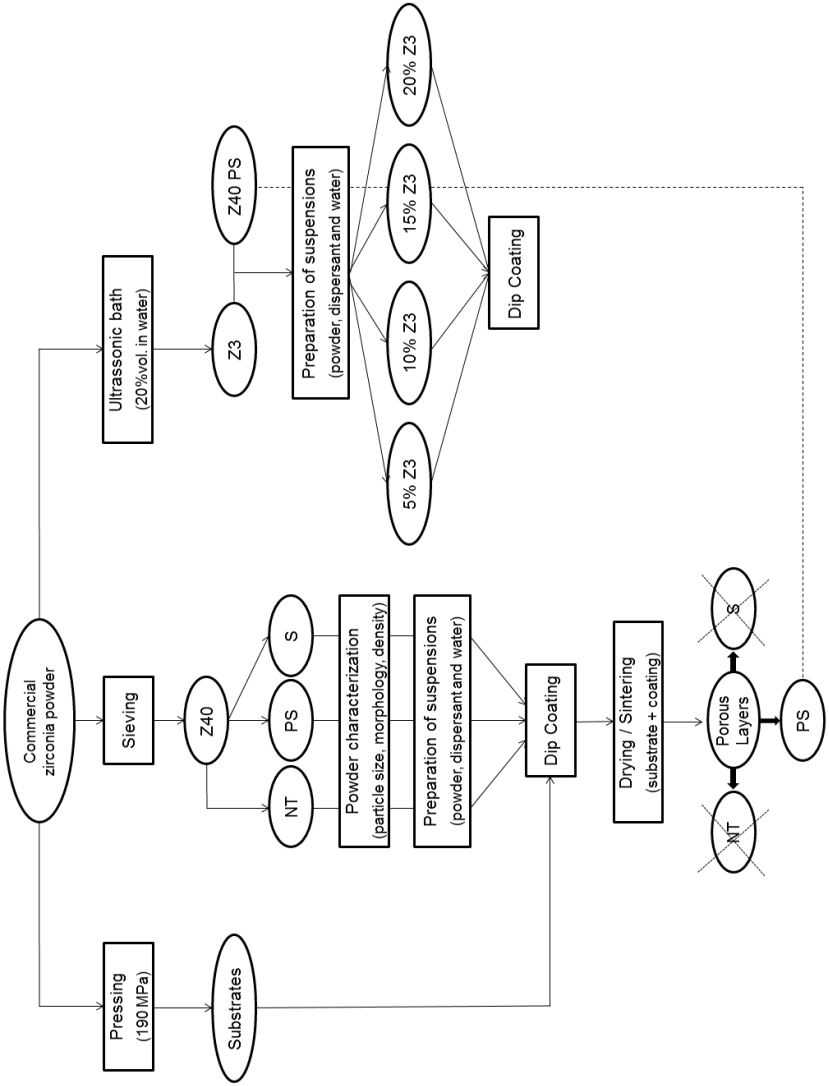

3.3. RESULTS AND DISCUSSION

Powder characterization

Figure 3.2 shows the particle size distribution of the commercial zirconia powder (as received), while Figure 3.2 shows the same material after heat treatments (PS and S) and sieving. The effect of temperature is remarkable: NT and PS powders show superposition of the curves, with a slight reduction in the "PS" size; S powders showed greater granule sizes (> 100 μm) among all tested conditions, probably due to a merge of small parts on greater volumes of agglomerates. A de-agglomeration process was needed after heat treatment of S powders to break the weak bonds between granules, generated by volumetric diffusion triggered by high temperature exposure (1500°C). The cumulative curve of the Figure 3.3 indicates a small difference between d_{50} of powders, with values around 42 μm for NT and PS powders, and 49 μm for S powders.

Figure 3.2 - Granule size distribution of commercial yttria-stabilized zirconia (TZ-3YBE).

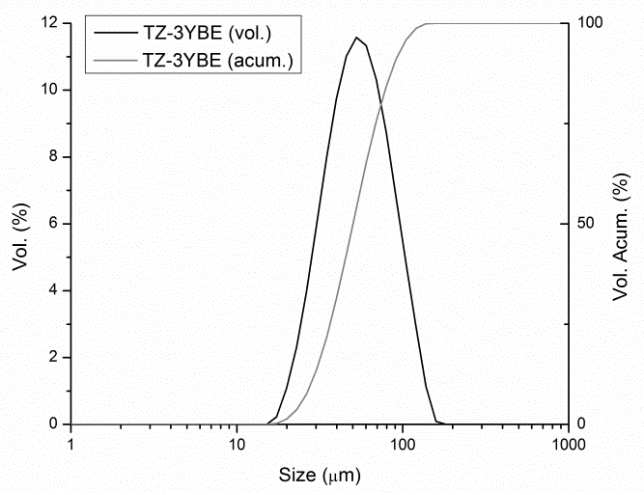

Figure 3.3 - Granule size distributions (solid line) and cumulative curve (dashed line) of Z40 powders with different heat treatments.

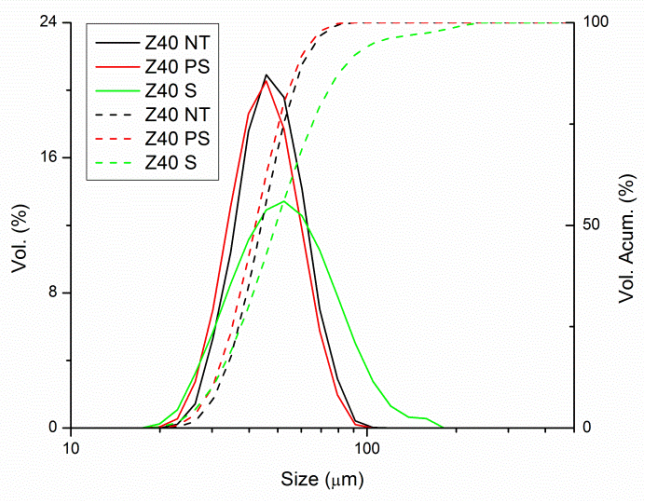

The morphology of the three groups can be observed in Figure 3.4, where the images confirm the mean sizes obtained from the particle size analyses. It is possible to observe the spherical shape in all groups of powders. The NT powders, however, presented some fractured agglomerates explained by the lower cohesive strength of powders in the absence of heat treatment. Greater consolidation of particles can be seen in PS and S groups, with homogeneous surfaces and less quantity of broken agglomerates. The heat treatment can influence the reactivity of surface by increasing atomic diffusion, leading to different densities of powders, as shown in the (REED, 1995).

It is important to emphasize the need to maintain the spherical morphology of agglomerates throughout the process, ensuring the formation of porosity through particle packing (MIAO; SUN, 2009).

Figure 3.4 - Z40 powders morphologies (NT, PS and S) and the respective vibrated density.

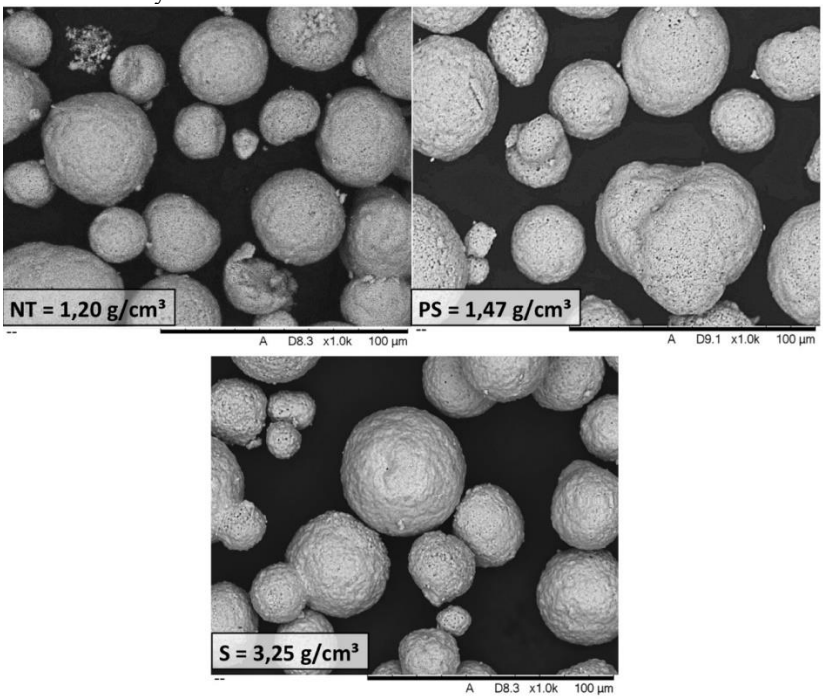

Dip coating with different suspensions

Figure 3.5 shows the particle size distributions of the suspensions with the different powders. A new peak below 10 µm of particle size was identified in NT suspension, meaning that the agglomerates undergone fragmentation during mixture of suspension. The distribution shifted from unimodal to bimodal. This phenomenon was not verified with the PS and S suspension, which underlines the higher cohesion reported previously in the SEM inspection of the different powders (Figure 3.4).

Figure 3.5 - Particle size distribution of Z40 suspensions: non thermal treated (NT), partially sintering (PS) and sintering (S).

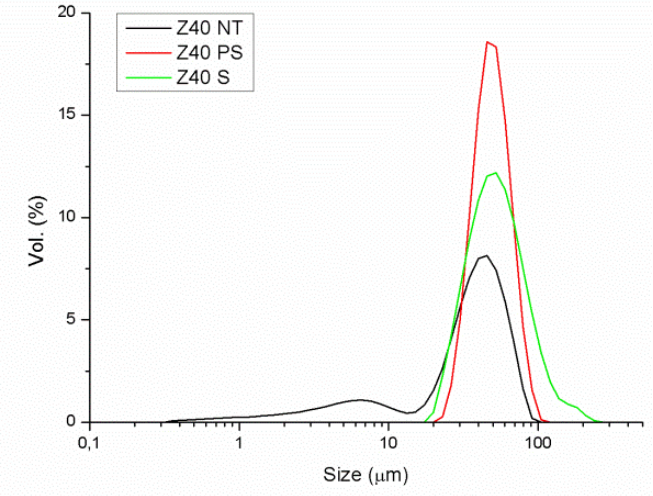

Figure 3.6 shows zirconia substrates dip coated with the different powders (NT, PS and S). It can be seen that NT layer does not present macroporosity and spherical particles, as seen in PS and S layers. The smeared shape of NT layer is supported by the particle size distribution curve plotted in Figure 3.5. Despite the undesired morphology, this layer showed good cohesion and adhesion to the substrate. On the other hand, layers formed by PS and S powders exhibited particles with spherical shape that were homogeneously distributed over the substrate, exhibiting the desired configuration of particles packing. The higher magnification of the PS layer micrograph, however, revealed the presence of small zirconia fragments within the spherical particles, working as bridges (necks) that could enhance the cohesion of the porous layer. These fragments were most probably traced back to the stirring process of the PS powders, which did not exhibit the maximum strength, as was the case of the S powders. It must be highlighted that no significant necks from solid-state diffusion were formed between the PS and S particles, which may compromise the mechanical strength of the coatings, due to a lack of consolidation between spherical granules of the layer. This lack of cohesion could be observed by the particles detachment, especially in the S layer. This fact lead us to consider a new approach to increase the mechanical strength of the porous layer. Therefore, taking as inspiration the observations

made in the NT layers, we decided to investigate the addition of fine particles (Z3) to the Z40-PS suspensions to simultaneously enhance the cohesion of the porous layers and its adhesion to the substrate. The particle size distribution of Z3 exhibited an average size of 3 µm (Figure 3.7). Small particles have the advantage of a greater superficial area, when compared to coarser ones, which induces a larger driving force for sintering.

Figure 3.6 - SEM of deposited layer using Z40 NT suspension (A), Z40 PS (B) and Z40 S (C).

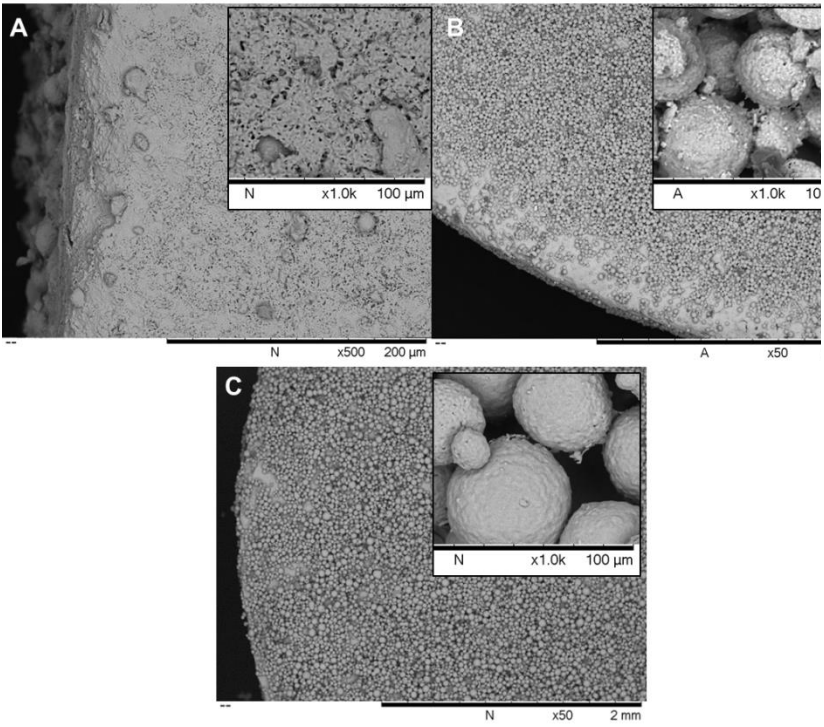

Figure 3.6-A shows the particle size distribution of suspensions with varied contents of fine particles. The presence of Z3 is evidenced by the peaks under 10 µm, which increases with greater contents of fine particles in the suspension. The viscosity analysis revealed a pseudoplastic behavior of the suspensions. Furthermore, the viscosity tended to decrease at a higher amount of Z3 particles. This behavior is in

accordance with Moreno (2005) that reported better flow of suspensions with wider particle size distributions at higher shear rates.

Figure 3.7 – (A) Particle size distribution of fine particles (Z3); (B) Size distribution of Z40 suspensions with the addition of different contents; and (C) viscosities as a function of the shear rate of the Z40 suspensions with the addition of several contents of Z3 particles.

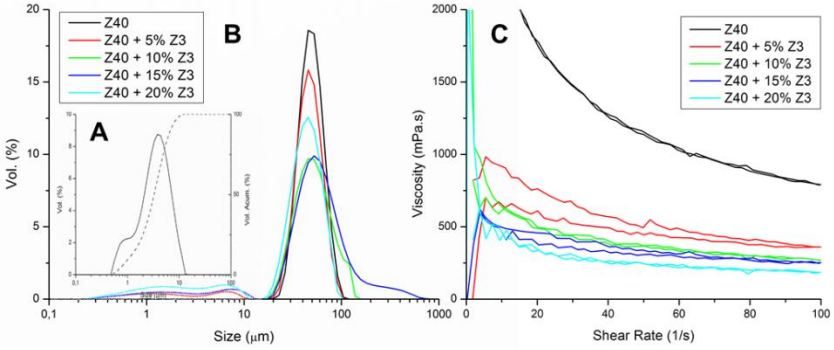

Figure 3.8 shows the micrographs of layers formed with PS powder plus different percentages of fine particles (Z3). The addition of 5% Z3 (Figure 3.8-a) showed no effect at the neck formation. Above 10% Z3, it is possible to note bonds between two or more Z40 particles, spread homogeneously over the layer. As the Z3 content increases it is possible to see the greater number of bonds within the particles, without significantly impacting the porosity and interconnectivity between the pores.

Figure 3.8 - SEM of layers containing Z40 plus: (a) 5% Z3; (b) 10% Z3; (c) 15% Z3 e (d) 20% Z3.

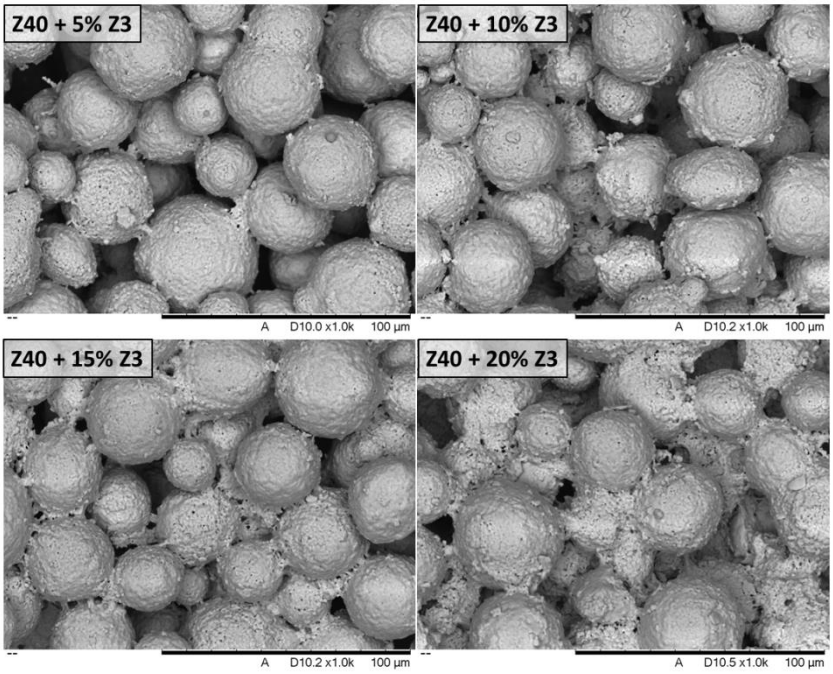

The influence of the addition of the Z3 particles on the cohesion of the porous layer was accessed by the wear test previously described, which results are plotted in Figure 3.9. It can be seen that the weight loss in the 5% Z3 sample was ~10 times higher the weight loss of the remaining samples, which highlights the lack of sufficient bonds between particles shown in Figure 3.8. The weight loss verified for contents above 10% Z3 dropped significantly, which evidences the beneficial effect of the Z3 particles as binding agents of the coarser particles.

Figure 3.9 - Weight loss of the Z40-coated zirconia substrates as a function of the fine particles (Z3) content in the dip coating suspension, during wear test.

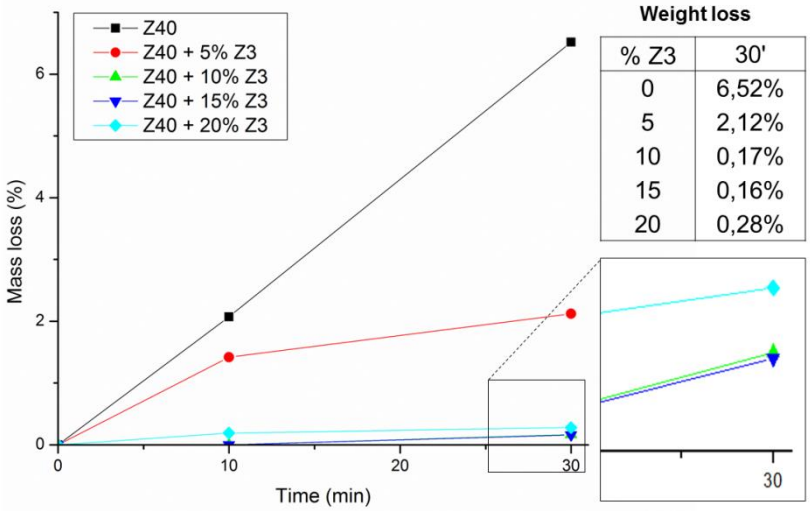

Weight loss

% Z3	30'
0	6,52%
5	2,12%
10	0,17%
15	0,16%
20	0,28%

Compression tests on porous solids made by slip casting, using the same suspensions of the dip coating process, confirm the tendency to increase strength of structures with addition of Z3, as seen in Figure 3.10. This resulted in the desired increase in the strength of the dip-coated layer. The specimen with 15% Z3 showed the lowest weight loss and, therefore, higher strength of deposited layer among all tested conditions. Figure 3.11 shows the top view and a cross-section view from the optimized layer of Z40, with thickness around 100 µm.

Figure 3.10 – Apparent porosity of porous solids varying Z3 content (left), and the respective compressive strength (right).

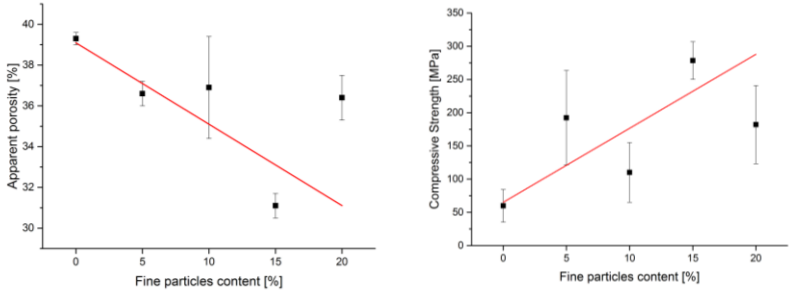

Figure 3.11 - Dip coated zirconia substrate with a suspension containing Z40+15%Z3 powders. The top view shows the open porosity and the particle bonding provided by the fine particles (Z3). The cross section view shows the Z40 particles piled up and a resulting thickness of ~100μm).

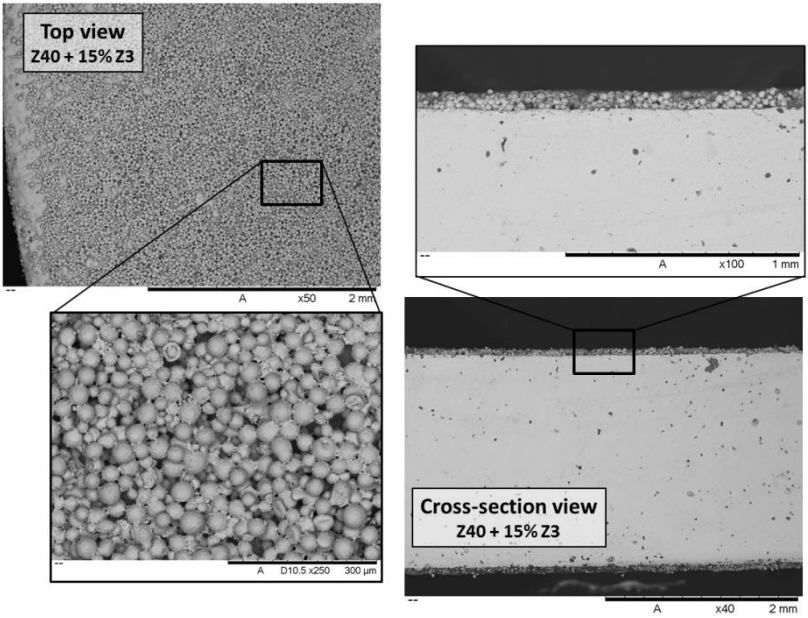

3.4. CONCLUSIONS

This work aimed at defining a processing route for producing surficial macroporous zirconia structures by the dip coating method. The following conclusions could be drawn:

- To produce porous layers by the dip coating method, the precursor powder must exhibit adequate cohesion to preserve the starting morphology during the whole dip coating process and thus allowing the formation of porosity at the particles packing interstices.
- A pre-sintering heat treatment of zirconia powders at 1150°C was found appropriate to maintain powder's spherical morphology during processing.
- The unimodal powder distribution, the powder size (Z40; ~40μm) and the zirconia sintering conditions (1500°C) resulted in the formation of weak bonds between the particles that formed the porous layer. To solve that, fine particles (Z3) of zirconia powders (~3 μm;

15% Z3) were successfully used as binding agent of the coarser particles, thus enhancing the cohesion of the particles composing the porous layers without affecting the connectivity of porosity.

* References at the end of the dissertation.

4. Optimization of porous layers route to obtain porous gradient on zirconia substrate by dip coating method

4.1. INTRODUCTION

Zirconia has been expanding its space in advanced ceramic applications since the mid-1970's, when the discovery of toughening mechanisms and increasing strength due to a phase transformation came to light. The need for the addition of stabilizers to control this transformation has opened up a range of new applications, depending on predominant structure of zirconia, influenced by the amount and main element of the additive. Yttrium oxide added to zirconia structures produce materials with superior mechanical properties such as high strength and flexibility, enough to compete with titanium alloys, besides being considered inert in contact with body, which allows its use as orthopedic implants, bone grafts, and dental restorations (DENRY; KELLY, 2008).

Structures of bones and teeth are natural examples of the so called functionally graded materials (FGM): the first case, a difference on the porosity between surface and core regions improves resistance to bending; and in the second case, by the dentin-enamel transition that links mechanical resistance of the nucleus (dentin) with chemical resistance of the surface (enamel). Natural teeth have the potential to last a lifetime, so the current implants try to mimic its structure to increase the useful life of specimens by reducing residual stresses from the contact between dissimilar materials, which is one of the main causes of early fracture (MEHRALI et al., 2013).

The gradient transition of properties, structures and/or compositions are designed to withstand different demands (mechanical, chemical, etc.) distributed along a section, and can be drawn to be at continuous or discrete format. Continuous transitions exhibit better properties although the process is expensive and complex; while discrete transition can be produced by deposition of successive layers that gradually changes its composition, forming a structure with transition bands (MIYAMOTO et al., 1999; UDUPA et al., 2014). The processing of layer depositions can vary in price, complexity and reproducibility, ranging from CVDs to coatings in general. Among these, the dip coating has the advantage of being a simple and low-cost technique, capable to cover a wide range of shapes. The deposition occurs by the immersion of a substrate in a suspension containing precursor material, which is incorporated into the surface via capillary forces. The thickness of the

layers is controlled by rheological conditions of suspensions and process parameters, such as speed and time of immersion (GROSSO, 2011; BRINKER, 2013).

The development of homogeneous or graded porous surfaces on biomaterials allows an improvement on osteointegration (as the case of cement-free implants) and also creates a favorable environment for the functionalization of this structure through impregnation or coating with of a second phase. For both applications, the pore size could range from 50 to 400 μm in order to optimize permeability of the layer and growth of natural tissues. Porosity also increases exposed surface area, which is convenient on interfaces structures (MIAO; SUN, 2009).

In this study, we report on the production of zirconia structures with surface macroporosity through the dip coating technique. Building up mono or multilayers of zirconia suspensions with different powders sizes allowed the production of homogeneous and graded macro surface porosity over the zirconia substrates. Practical examples as to these porosities may be applied are given in the end of the paper.

4.2. MATERIALS AND METHODS

Production of surface homogeneous macroporosity

The base material of this study was a 3% mol yttria-stabilized zirconia spray-dried powder (TZ-3YBE, TOSOH Co., Tokyo, Japan). This commercial powder, formed by spherical agglomerates with average size of 60 μm and green density of 1,1 g/cm³, was used in two different forms: pre-sintered powders and as fine particles. The pre-sintered powders underwent a heat treatment at 1150°C for 1 h for consolidation of the starting agglomerates. They were afterwards sieved to obtain narrower size distributions, forming three groups of particles with average sizes of 40, 70 and 100 μm, hereafter referred as Z40, Z70 and Z100, respectively (Figure 4.1). The fine powders were obtained from a sonication process of the commercial powders for de-agglomeration, thus resulting in particle sizes of approximately 3 to 10 μm, hereafter referred as Z3 (Figure 4.1). The F particles did not undergo heat treatment. All size distribution analyses were made in Mastersizer 2000 (Malvern) equipment.

Measurements of density were made by analysis of volume of powder occupied in a test tube (pycnometry), and its respective mass. It

was necessary to vibrate the test tube for 3 minutes, in order to accommodate particles compactly.

Figure 4.1 - Particle size distribution of (a) the three groups of "coarse" zirconia used as base materials; and (b) fine particles.

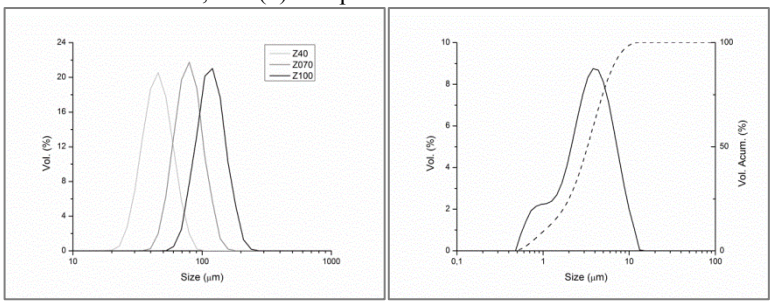

All ceramic suspensions were prepared with 30 vol.% of solid content and 2 m.% of the suspending agent CMC (carboxymethylcellulose) (Emfal, Betim, Brazil), in reference to total solid mass. The solid contents of the suspensions were composed by a mixture of coarse and fine powders: Z40-15% Z3, Z70-25%Z3 and Z100-25%Z3 (relation to volume). The fine particles contents in the different suspensions were determined based on previous experiments.

The dip coating was made over uniaxially pressed commercial zirconia discs (150 MPa), non-sintered, with 20 mm of diameter and 2 mm height. The layers build up on zirconia substrates followed the next sequence: discs were first dipped into Z3 suspension to form a thin adhesive layer between the substrate and the upper coarse powder layer. The first dipped layer of Z3 powders dried in air before receiving the next layer of coarser particles. During experimental work, it was found the need to perform in multilayered specimens intermediate heat treatments to the freshly deposited layers in order to avoid the layers leaching to the suspension. Three treatments were tested: air drying, muffle kiln and pre-sintering (1150°C), with the latter being the most efficient in maintaining the layers morphology. Therefore, specimens with homogeneous surface porosity were produced with one, two and three dips (in the same suspension), passing through a pre-sintering treatment between each dip (Appendix A).

After the build-up of the last layer, the specimens were air-dried and air sintered in a conventional furnace at 1500°C for 2h. Scanning electron microscopy (SEM) (TM3030, Hitachi, Japan) was used to

analyze the microstructure of the different specimens. Specimens were gold coated prior to SEM inspection.

Production of surface graded macroporosity

To produce the gradient of macroporosity at the surface of zirconia discs, a sequence of layers was deposited, following the same steps mentioned above for the production of homogeneous porosity: a layer of Z3 particles is first deposited followed by a sequential deposition of smaller to bigger powders, using Z40, Z70 and Z100 suspensions, respectively. Two conditions were tested: a single sequential dip in each suspension (Z40 + Z70 + Z100), condition referred as Grad SD; and double sequential dip in each suspension (2xZ40 + 2xZ70 + 2xZ100), referred as Grad DD. It must be referred that both Grad SD and Grad DD specimens underwent a preliminary dip of Z3 prior to coarse powders layers, similarly to the above described for specimens with homogenous porosity. The specimens were finally air sintered at 1500°C for 2h.

Porous solids by slip casting

In order to characterize the mechanical properties of the porous layers tested in this study, porous solids with cylindrical shape were produced from the same suspensions used to produce the porous coatings in the zirconia discs, using the slip casting technique (Appendix B). Despite they are different techniques, slip casting was found to have high similitude to dip coating, thus allowing to produce porous solids with properties close to the layers produced over the zirconia substrates. Hence, several cylindrical porous solids were produced using a polymer mold (13 mm of diameter and 30 mm height) with an absorbent base attached. Suspensions with coarse powders (Z40, Z70 and Z100) and varying Z3 contents (20, 30, 40 and 50vol%) were tested. Suspensions were poured into the mold, drained by the absorbent base, and dried in a stove for 48 h. The specimens showed different height, but the h/D relation remains between 0.3 and 1.5 according to ASTM C133-97 (for compressive tests). The specimens were polished to ensure parallelism between faces, and then, sintered at 1500°C/2h. Structures were analyzed via SEM as regard to their morphology, porosity and connectivity of pores.

The apparent porosity was measured using ASTM C20-00, by weighing of the specimens under three conditions: D – dry; I –

immersed in water; and W – wet (saturated with water, removed drops from the surface). The apparent porosity (%) expresses the volumetric relation of open pores to external volume. Apparent density (g/cm³) represents the quotient of the dry weight divided by the total volume, including pores. All calculations consider water density as 1 g/cm³, and sintered zirconia (theoretical) as 6.05 g/cm³.

$$P\ (\%) = \frac{(W-D)}{(W-I)}.100 \qquad \text{(Equation 4.1)}$$

$$\rho_{ap}\ (g/cm^3) = \frac{D}{(W-I)} \qquad \text{(Equation 4.2)}$$

Mechanical characterization

The fracture strength of coated specimens was obtained from a ball-on-three-balls test (B3B) performed in a universal testing machine (Instron 8874, MA, USA), especially used for testing disc shaped specimens of britlle materials. The specimens were loaded under a crosshead speed of 0.15 mm/s until its rupture, using a load cell of 25 kN. The strength is the force applied at the first "break" of the specimen (ZIELKE et al, 2016).

The fracture surfaces were then inspected by SEM in order to assess the influence of the biaxial test on the fracture pattern and integrity of the porous coatings.

The mechanical properties of the porous coatings were estimated by the assessment of the compressive strength of porous solids produced by slip casting. Tests were conducted in a universal testing machine (Emic DL 2000) with load cell TRD 27 (200 kN) and loading speed of 0.5 mm/min.

4.3. RESULTS AND DISCUSSION

Characterization of homogeneous macroporous layers

The comparison of morphologies of treated (pre-sintered) and untreated Z100 powders can be seen in Figure 4.2. Treated powders (PS) exhibit consolidated surfaces with higher cohesion than the non-treated (NT), evidenced by the spherical shape and the absence of fractured agglomerates. This allows the agglomerates to keep its original shape during the stirring processes associated to the preparation of

suspensions for the dip coating process. The heat treatment imparts to the powders a slight increase in density (~20%) relative to non-treated ones: 1.20 $g.cm^{-3}$ for non-treated (NT) powders and 1.47 $g.cm^{-3}$ for pre-sintered (PS) powders.

In the previous chapter, addition of fine powders to the coarser powders suspensions was necessary for increasing cohesion of the macroporous layers deposited over zirconia substrates.

Figure 4.3 compares morphologies of two Z40 layers (a) with no addition of Z3 particles, and (b) with addition of 15% (vol.%) of Z3 particles. It is clearly seen the beneficial effect of the fine particles in terms of setting bonds between the coarser particles without significantly compromising the interconnectivity between them. The relation of fine particle (Z3) to coarse particles (Z40) content have been previously optimized (in the previous chapter) as regard to the layer's morphologies with varying Z3 contents, porosity and compressive strength of "layers" (porous solids with similar compositions).

Figure 4.2 - SEM of Z100 powder (a) treated at 1150°C and (b) untreated.

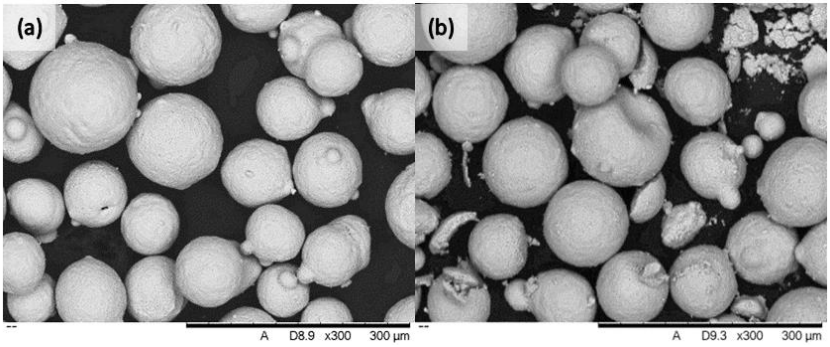

Figure 4.3 – Top view of zirconia layers produced by dip coating using Z40 suspensions: a) no addition of fine particles (Z3) to Z40 suspension; b) addition of 15% Z3 to the Z40 suspension.

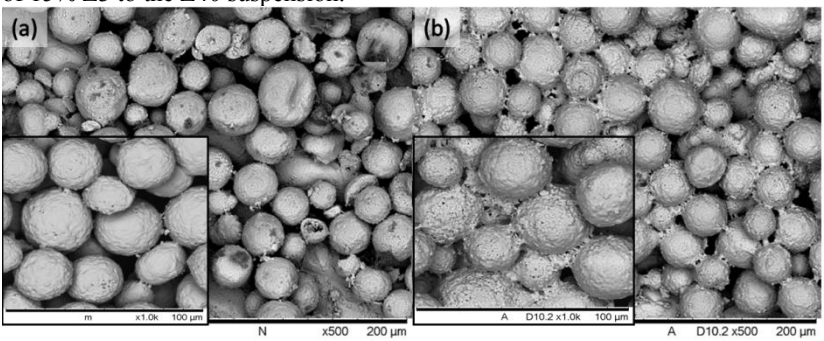

As stated before, the porous solids structures made by slip casting may differ in some extent to the layers deposited by dip coating. Nevertheless, due to the similar packing arrangement of both processes, this process was selected for producing the porous solids that allowed estimating the porosity and compressive strength of the dip coated layers. The porous solids revealed a decreasing trend of porosity for increasing contents of Z3 particles in the suspensions, regardless of the coarse powder size (Z40, Z70 or Z100), as depicted in Figure 4.4 and further evidenced in density measurements presented in Table 4.1.

Density values follow the opposite trend, with higher contents of Z3 particles producing denser solids. Coarser powders combined with Z3 particles show higher densities results in improved packing efficiency – a greater difference on the diameters of the components influences negatively in the point of view of forming porosity, as Oliveira's graphs indicates (OLIVEIRA et al., 2000) due to a more compact packing arrangement. Additionally, higher densities impart greater mechanical strength and stiffness to porous solids since porosity is regarded reducing the Young's modulus of the system.

Figure 4.4 - Influence of fine particles content on the apparent porosity of porous solids produced by slip casting using suspensions containing coarse powders (Z40, Z70 or Z100) and different amounts of fine particles (Z3) contents.

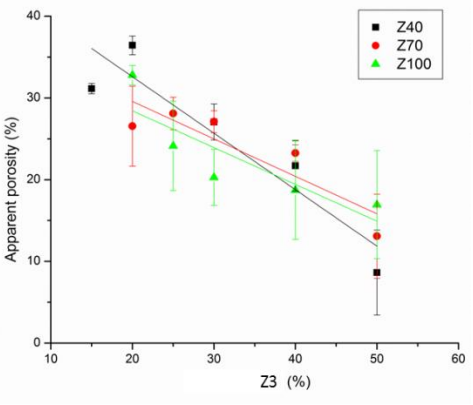

Table 4.1 – Density measurement (g.cm^{-3}) of porous solids, made by slip casting, of Z40, Z70 and Z100 specimens.

% Z3	Z40	Z70	Z100
20	3.38 ± 0.04	3.82 ± 0.30	3.57 ± 0.17
30	3.60 ± 0.14	3.61 ± 0.09	4.20 ± 0.17
40	3.97 ± 0.08	3.93 ± 0.16	4.23 ± 0.46
50	3.96 ± 0.87	4.45 ± 0.23	4.86 ± 0.92

Figure 4.5 shows the compressive strength of the porous solids made of different powder sizes (Z40, Z70 and Z100) as a function of the fine particles (Z3) contents in the suspensions. It can be seen that strength increases with the increasing content of Z3 particles and that this effect was more pronounced for particles of bigger size.

Figure 4.6 shows the single- and double-dipped zirconia substrates with Z40, Z70 and Z100 powders. It can be clearly seen from the image the effect of particle size as well as the number of dips. A single-dip was not able to cover the edges of the substrate regardless the size of the powder. When two dips were performed, the Z40 and Z70 suspensions a full coverage of the edges of the specimens was achieved. The same effect was only obtained for Z100 specimens after the third dip coating.

Figure 4.5 - Compressive strength (MPa) of the porous solids produced by slip casting, varying Z3 content.

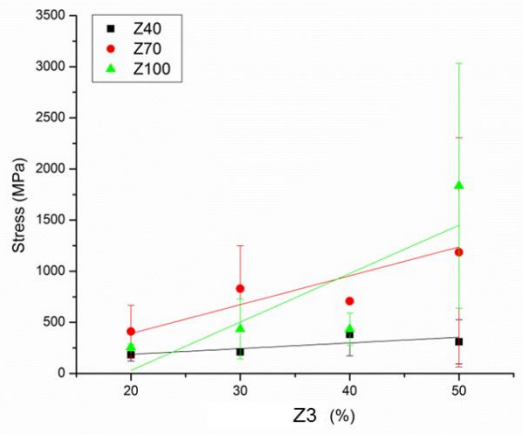

Figure 4.6 - SEM of layers formed by a single dip (first line) and double dip (second line) in suspensions: Z40-15%Z3 (left), Z70-25%Z3 (middle) and Z100-25%Z3 (right). The smaller images show a larger magnification (x1000) of the respective system (column), with the focus of showing the connections between coarser particles.

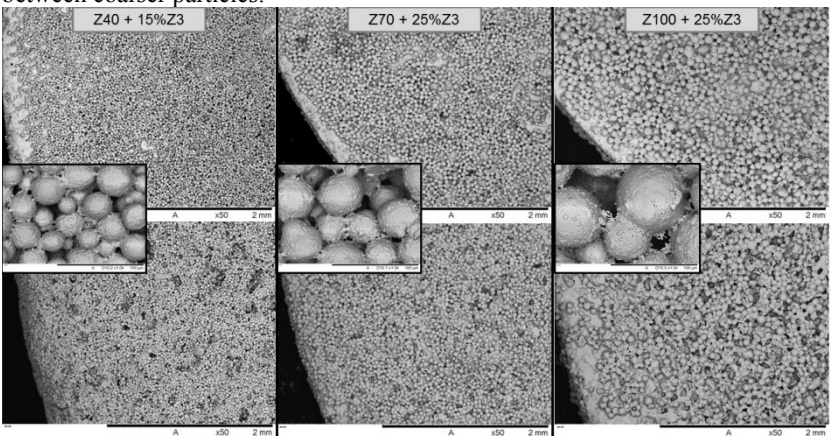

As the number of dips increases, it becomes more difficult to control thickness due to excessive formation of bubbles on the surface in some substrates. Two possible causes can be advanced: insufficient time for the liquid to penetrate the surface porosity, and the viscosity of the suspension, which can also affect the time required to complete

"absorption" of the liquid. High viscosity can also form thick droplets, especially at the edges, causing heterogeneities in the layers. Immediately drying of the substrate after its withdraw from suspension may avoid gross marks on the deposited surface, but it does not eliminate the formation of irregularities.

Figure 4.7 shows SEM micrographs of the cross section view of different specimens produced in this study. The thickness of each specimen is marked with dashed line for guidance of the reader, as the depth effect resulting from specimens tilting during observation may be misleading regarding the real thickness value. The thicknesses values measured on different specimens were recorded and exhibited in Figure 4.8. The coating thickness was found to vary linearly with the number of dips for all the powder sizes. Comparing the three systems, the single-dip Z40 layer exhibited the best particle packing, since its average thickness was equivalent to overlap 2.7 particles of Z40, higher than Z70 and Z100 layers, with average thicknesses similar to 1.6 "overlapped" particles (considering respective mean size of each system).

Figure 4.7 - SEM micrograph of the cross-section view of the Z40, Z70 and Z100 layers formed by one, two and three dips.

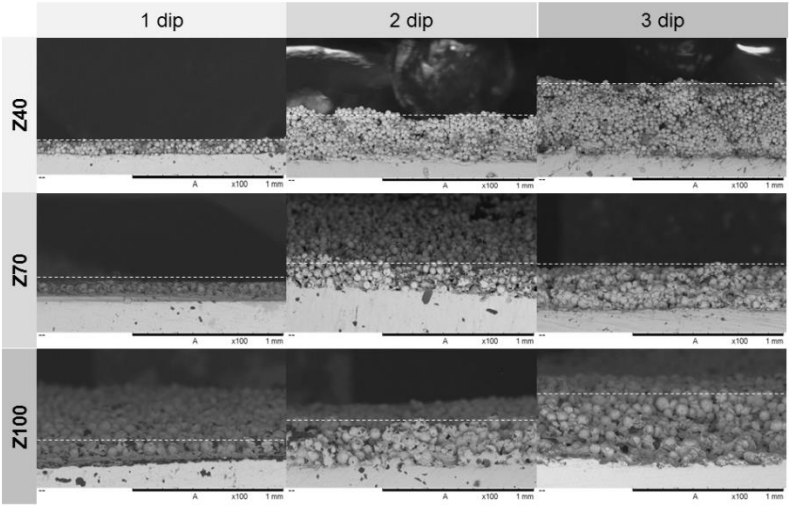

Figure 4.8 - Layer evolution with number of dips.

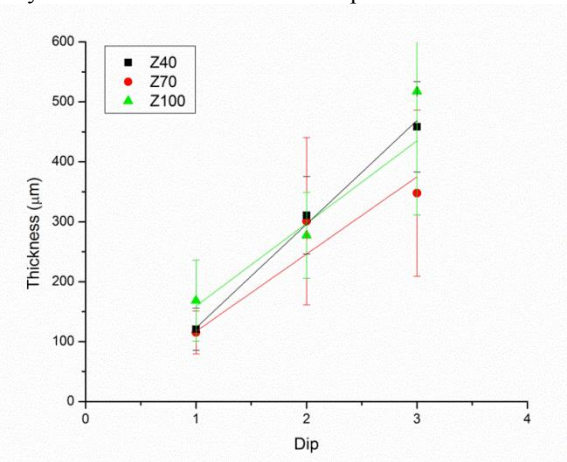

Biaxial strength tests

Dip coated specimens were subjected to biaxial strength tests (B3B) to assess the influence of the macroporous coatings on the flexural strength of the zirconia substrates. Figure 4.9 shows the results obtained from the B3B test of the coated specimens, as well as of the uncoated specimens for reference. It can be seen that, regardless of the type of coating, the fracture loadings of coated specimens were above the results obtained for the uncoated specimens, taken as the "control group" (1500 ± 190 N), mean value indicated by the dashed line and the gray area represents the standard deviation. This means that the presence of macroporous coatings did not induce a detrimental effect on the fracture resistance of the zirconia specimens, as could be initially supposed based on the higher surface roughness imparted by porous coatings. The results obtained from static load to fracture tests may therefore present a different trend under fatigue conditions. Therefore, further studies should be conducted to suitably address this issue.

Figure 4.9 – Fracture strength of the surficial macroporous zirconia specimens obtained from B3B test: fracture load (N) versus the number of dip coatings (1x, 2x, 3x) with different suspensions (Z40, Z70 and Z100).

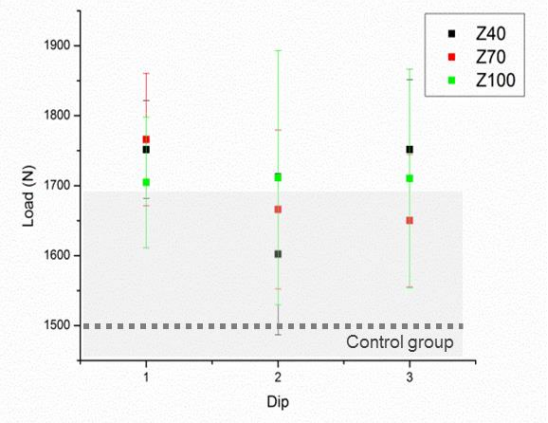

Figure 4.10 shows the fracture surface of the Z40 and Z100 specimens with single-dip coating, and Z70 double-dipped specimen, with an arrow indicating the loading point at the compressive surface. The compressive curls are well evidenced at this adjacent region. Delamination occurrences of the porous layers were seen in specimens subjected to the flexural test (B3B), with thicker layers being more prone to this phenomenon. Hence, single-dipped specimens showed few or no delamination of layers; whereas specimens with double and triple dipped layers exhibited greater occurrences.

Figure 4.10 - Fracture surface of Z40 (single-dip), Z70 (double-dip) and Z100 (single-dip) specimens.

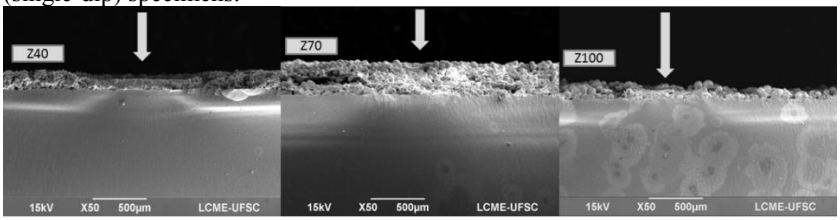

A double-dipped Z40 layer after B3B test is seen in Figure 4.11, in which the beginning of the delamination is visible as a propagation of the stress zone: the yellow arrow represents direction of loading, while dark arrows, the direction of delamination. The white dashed arrow indicates the fracture origin at the tensile surface of the specimen.

The delamination trend during flexural test was exhibited by all groups as seen in Table 4.2. However, thicker coatings and bigger particles presented higher delamination incidence.

Figure 4.11 – Z40 double-dipped layer: cross-section of a fractured specimen (above) and a non-tested sample (below).

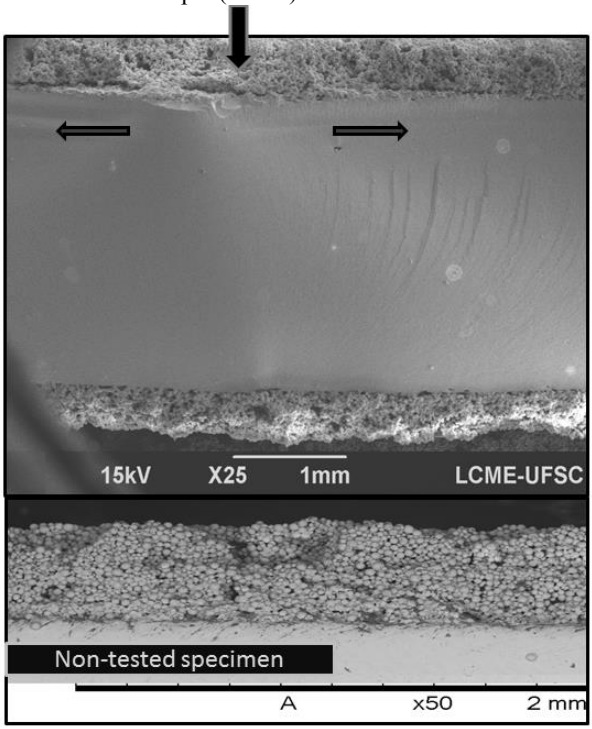

Table 4.2 - Percentage of delaminated specimens after B3B test (considering any sign of delamination).

	1 dip	**2 dip**	**3 dip**
Z40	18 %	36 %	70 %
Z70	-	30 %	60 %
Z100	10 %	40 %	70 %

Characterization of graded macroporous layers

Figure 4.12 shows the cross-section view of layers deposited by the consecutive immersion in suspensions with Z40, Z70 and Z100 powders. In Figure 4.12-A, the graded porous layer was obtained by a single dip in each suspension (Z40 + Z70 + Z100), making a total of three dips. In Figure 4.12-B, the graded porous layer was produced by dipping twice in each suspension (2xZ40 + 2xZ70 + 2xZ100), making a total of 6 dips. The thickness is the main difference among the structures: Grad SD with average values around 300 ± 50 μm, and Grad DD around 660 ± 240 μm. The detailed view of the graded coating profiles is seen in Figure 4.12 from the high magnification micrographs, where the dash lines indicate the average bands of each zirconia powders.

Table 4.3 presents the fracture load values obtained for Grad SD and Grad DD specimens (n ~ 10). The fracture load of both specimens remained within the same range of the values obtained for specimens with homogeneous porous layers (increase ~20%), which means that the thickness of layers and the number of dips did not seem to compromise the static fracture resistance. Nevertheless, the same concerns regarding the fatigue behavior mentioned above for specimens with homogeneous porous layers, also applies for Grad SD and Grad DD specimens.

Figure 4.12 - Layer formed with sequential dip in Z40, Z70 and Z100 suspensions: (a) Grad SD – single-dipped on each group, (b) Grad DD – double-dipped.

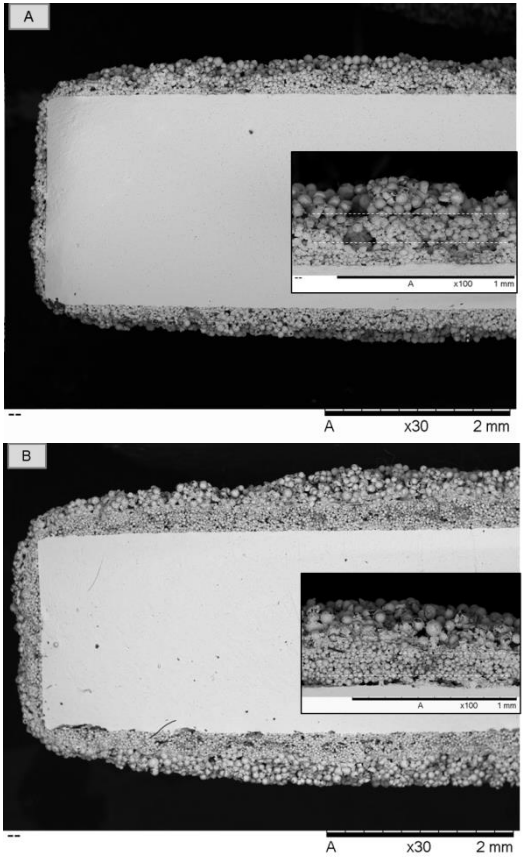

Table 4.3 - Measured values of the layer's thickness, total specimens thickness and fracture load (N) after B3B test for the specimens with graded macroporous coatings: Grad SD and Grad DD.

	Layer Thickness (µm)	**Specimen Thickness (mm)**	**Fracture Load (N)**
Grad SD	290 ± 40	2,71 ± 0,05	1808,7 ± 97,3
Grad DD	750 ± 220	3,93 ± 0,41	1741,1 ± 200,5

The occurrence of delamination was also verified in the case of gradient layers, as shown in Figure 4.13. All Grad DD samples presented delaminated layers after test, while only 25% of Grad SD samples showed this phenomenon, exhibiting the same trend previously seen for specimens with homogeneous porous coatings.

Figure 4.13 – Delaminated layers of Grad SD (left) and Grad DD systems (right) after flexural tests (B3B).

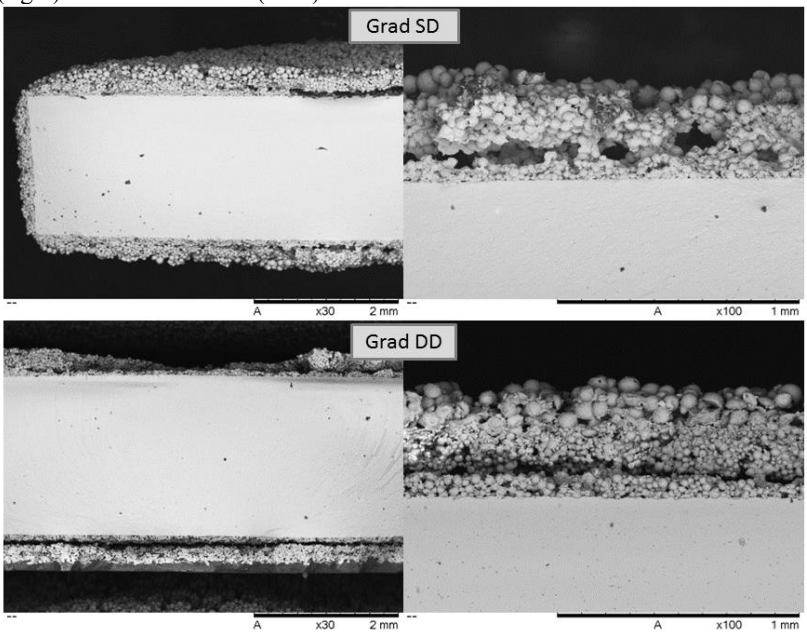

4.4. CONCLUSIONS

This work aimed to produce and characterize homogeneous and graded macroporous zirconia layers over zirconia substrates by the dip coating technique. The following conclusions could be drawn:

- Homogeneous and graded macroporous layers were successfully built over zirconia substrates using suspensions with powders of different sizes (Z40, Z70, Z100 and fine particle (Z3)), using the dip coating technique.
- The thickness of the porous layer increased with the increasing number of dips, regardless the size of the powder (Z40, Z70, Z100).

- The fracture strength of the specimens with homogeneous and graded macroporous layers was higher than that of uncoated specimens (~20%), meaning that coatings were not detrimental for the static strength of the porous specimens.
- The flexural tests imparted delamination occurrences in the porous layer of some specimens, with the higher incidence being observed for coatings with larger thicknesses and bigger particles/granules.

5. GENERAL CONCLUSIONS & SUGGESTIONS

5.1. CONCLUSIONS

The investigation on the route of fabrication of surface porous layers of zirconia presented as main conclusions:

- The powders must remain spherical throughout the processing in order to generate the expected interstices. For this, heat treatment of the starting material is required;
- A better cohesion of the layer is achieved by adding fine particles to the system, acting as binder agent for coarser particles;
- A "pre-deposition" of fine particles (<10 μm) on the substrate is necessary for improved adhesion among substrate and successive layers;
- Homogeneous and graded layers were feasible to be produced by successive depositions over the substrate, although studies related to the drying and heat treatment between depositions should be further investigated;
- Fracture strength of both layers, homogeneous and graded, were higher than uncoated substrates;
- Flexural tests evidence delaminations of the porous layers in some specimens, increasing incidence on larger thickness layers.

5.2. SUGGESTIONS

During this study, some points of the process indicate the need of improvement, suggesting that future works should study:

- An investigation on the effect of drying on the layers, considering multiple depositions, in order to avoid delaminations and drying defects;
- Estimate residual stresses of porous solids (slip casting) after burn-out by dilatometry;
- A study of the impregnation with porcelain and/or bioglass on graded and homogeneous layers structures for biomedical applications;
- A study of interconnectivity of pores, on layer, and a complex analysis of the thickness to obtain a ;
- Mechanical characterization of the samples (both homogeneous and graded porous layers) under humidity and cyclic loadings for biomedical applications;
- Characterization for biomedical applications: *in vitro* and *in vivo*.

REFERENCES

ALBINO, M. P.; GARRIDO, L. B. Effect of zirconia tape porosity on fluorapatite surface film formation by dip coating. Ceramics International, v. 39, p. 29-37, 2012.

AMERICAN SOCIETY FOR TESTING AND MATERIALS. C133-97: Standard Test Methods for Cold Crushing Strength and Modulus of Rupture of Refractories. Vol. 15.01.

AMERICAN SOCIETY FOR TESTING AND MATERIALS. C20-00: Standard Test Methods for Apparent Porosity, Water Absorption, Apparent Specific Gravity, and Bulk Density of Burned Refractory Brick and Shapes by Boiling Water. Vol. 15.01.

BARANI, A.; BUSH, M. B.; LAWN, B. R. Effect of property gradients on enamel fracture in human molar teeth. Journal of the mechanical behavior of biomedical materials, v. 15, p. 121–30, 2012. Available on: <http://www.sciencedirect.com/science/article/pii/S175161611200183X>. Date of access: 13/10/2015.

BLAESE, D. Processing and characterization of monoclinic-zirconia fibre-matrix interfaces in dense matrix alumina-alumina composites [dissertação]. Florianópolis: Universidade Federal de Santa Catarina, Programa de Pós-Graduação em Engenharia Mecânica; 2013.

BOCCACCINI, A R.; KEIM, S.; MA, R.; LI, Y.; ZHITOMIRSKY, I. Electrophoretic deposition of biomaterials. Journal of the Royal Society, Interface / the Royal Society, v. 7 Suppl 5, n. May, p. S581–S613, 2010.

BRINKER, C. J. Dip Coating. In: T. Schneller et al. (eds.), Chemical Solution Deposition of Functional Oxide Thin Films. Albuquerque: Springer-Verlag Wien; p. 233–261, 2013. Available on: <http://link.springer.com/10.1007/978-3-211-99311-8>.

CAMILO, C. C. Implantes de alumina em gradiente funcional de porosidade recobertos com hidroxiapatita e biovidro: avaliação da osseointegração [tese]. São Carlos: Universidade de São Paulo, Departamento de Engenharia Mecânica - Escola de Engenharia de São Carlos; 2010.

CASTRO, A. L. DE; PANDOLFELLI, V. C. Revisão: Conceitos de dispersão e empacotamento de partículas para a produção de concretos especiais aplicados na construção civil. Cerâmica, v. 55, n. 333, p. 18–32, 2009.

CHEVALIER, J. What future for zirconia as a biomaterial? Biomaterials, v. 27, n. 4, p. 535–43, 2006. Available on:

<http://www.sciencedirect.com/science/article/pii/S0142961205007039>. Date of access: 26/2/2015.

COLOMBO, P.; SCHEFFER, M. Cellular Ceramics: Structure, Manufacturing, Properties and Applications. Michigan: Wiley; 2005.

CONCEIÇÃO, E. S. Influência da distribuição granulométrica no empacotamento de matérias- primas na formulação de porcelânicos [dissertação]. São Paulo: Universidade de São Paulo, Programa de Pós-Graduação do Departamento de Engenharia Metalúrgica e de Materiais; 2011.

DENRY, I.; HOLLOWAY, J. A. Ceramics for dental applications: A review. Materials, v. 3, n. 1, p. 351–368, 2010.

DENRY, I.; KELLY, J. R. State of the art of zirconia for dental applications. Dental materials : official publication of the Academy of Dental Materials, v. 24, n. 3, p. 299–307, 2008. Available on: <http://www.sciencedirect.com/science/article/pii/S0109564107001133>. Date of access: 11/8/2015.

GROSSO, D. How to exploit the full potential of the dip-coating process to better control film formation. Journal of Materials Chemistry, v. 21, n. 43, p. 17033, 2011.

GU, Y.; MENG, G. A model for ceramic membrane formation by dip-coating. Journal of the European Ceramic Society, v. 19, n. 11, p. 1961–1966, 1999. Available on: <http://www.sciencedirect.com/science/article/pii/S0955221999000138>. Date of access: 26/9/2015.

HANNINK, R. H. J.; KELLY, P. M.; MUDDLE, B. C. Transformation Toughening in Zirconia-Containing Ceramics. Journal of the American Ceramic Society, v. 83, n. 3, p. 461–487, 2000.

HEDIA, H. S.; MAHMOUD, N.-A. Design optimization of functionally graded dental implant. Bio-medical materials and engineering, v. 14, n. 2, p. 133–143, 2004.

JAMALUDIN, A. R.; KASIM, S. R.; ABDULLAH, M. Z.; AHMAD, Z. A. Physical, mechanical, and thermal properties improvement of porous alumina substrate through dip-coating and re-sintering procedures. Ceramics International, v. 42, p. 7717–7729, 2015.

KELLY, J.; BENETTI, P. Ceramic materials in dentistry: historical evolution and current practice. Australian Dental Journal, v. 56, p. 84–96, 2011. Available on: <http://doi.wiley.com/10.1111/j.1834-7819.2010.01299.x>. .

KELLY, J. R. Clinically relevant approach to failure testing of all-ceramic restorations. The Journal of Prosthetic Dentistry, v. 81, n. 6, p. 652–661, 1999. Available on:

<http://www.sciencedirect.com/science/article/pii/S0022391399701034>. Date of access: 19/10/2015.

KELLY, J. R.; DENRY, I. Stabilized zirconia as a structural ceramic: an overview. Dental materials : official publication of the Academy of Dental Materials, v. 24, n. 3, p. 289–98, 2008. Available on: <http://www.sciencedirect.com/science/article/pii/S0109564107001121>. Date of access: 25/8/2015.

KHANUJA, H. S. Cementless Femoral Fixation in Total Hip Arthroplasty. The Journal of Bone and Joint Surgery (American), v. 93, n. 5, p. 500, 2011. Available on: <http://jbjs.org/cgi/doi/10.2106/JBJS.J.00774>. .

KOZUKA, H.; YAMANO, A.; FUJITA, M.; UCHIYAMA, H. Aqueous dip-coating route to dense and porous silica thin films using silica nanocolloids with an aid of polyvinylpyrrolidone. Journal of Sol-Gel Science and Technology, v. 61, n. 2, p. 381–389, 2012.

LAWSON, S. Environmental degradation of zirconia ceramics. Journal of the European Ceramic Society, v. 15, n. 6, p. 485–502, 1995. Available on: <http://www.sciencedirect.com/science/article/pii/095522199500035S>. Date of access: 19/10/2015.

LENORMAND, P.; CARAVACA, D.; LABERTY-ROBERT, C.; ANSART, F. Thick films of YSZ electrolytes by dip-coating process. Journal of the European Ceramic Society, v. 25, n. 12 SPEC. ISS., p. 2643–2646, 2005.

LUGHI, V.; SERGO, V. Low temperature degradation -aging- of zirconia: A critical review of the relevant aspects in dentistry. Dental materials : official publication of the Academy of Dental Materials, v. 26, n. 8, p. 807–20, 2010. Available on: <http://www.sciencedirect.com/science/article/pii/S0109564110001132>. Date of access: 6/8/2015.

LUO, J.; ADAK, S.; STEVENS, R. Microstructure evolution and grain growth in the sintering of 3Y – TZP ceramics. Journal of materials science, v. 33, p. 5301–5309, 1998.

MAIA, D. F. Desenvolvimento de Membranas Cerâmicas para Separação de Óleo/Água [Tese]. Campina Grande: Universidade Federal de Campina Grande, Programa de Doutorado em Engenharia de Processos; 2006.

MANICONE, P. F.; ROSSI IOMMETTI, P.; RAFFAELLI, L. An overview of zirconia ceramics: basic properties and clinical applications. Journal of dentistry, v. 35, n. 11, p. 819–26, 2007.

MARTIN, P. M. Introduction to Surface Engineering and Functionally Engineered Materials. Salem: Wiley; 2011.

MATIAS, E. M. Obtenção de materiais cerâmicos com gradiente de porosidade, utilizando-se a técnica de colagem de barbotina [dissertação]. São José dos Campos: Universidade do Vale do Paraíba, Programa de Pós- Graduação em Engenharia Mecânica; 2007.

MCENTIRE, B. J.; BAL, B. S.; RAHAMAN, M. N.; CHEVALIER, J.; PEZZOTTI, G. Ceramics and ceramic coatings in orthopaedics. Journal of the European Ceramic Society, v. 35, n. 16, p. 4327–4369, 2015. Available on: <http://dx.doi.org/10.1016/j.jeurceramsoc.2015.07.034>. .

MEHRALI, M.; SHIRAZI, F. S.; MEHRALI, M.; et al. Dental implants from functionally graded materials. Journal of Biomedical Materials Research Part A, v. 101, n. 10, p. 3046–3057, 2013. Available on: <http://doi.wiley.com/10.1002/jbm.a.34588>. .

MIAO, X.; HU, Y.; LIU, J.; HUANG, X. Hydroxyapatite coating on porous zirconia. Materials Science and Engineering **C**, v. 27, n. 2, p. 257–261, 2007.

MIAO, X.; SUN, D. Graded/Gradient Porous Biomaterials. Materials, v. 3, n. 1, p. 26–47, 2009. Available on: <http://www.mdpi.com/1996-1944/3/1/26/>. .

MIYAMOTO, Y.; KAYSSER, W. A.; RABIN, B. H.; KAWASAKI, A.; FORD, R. G. Functionally graded materials: design, processing and applications. Springer: 1999.

MIYAZAKI, T. et al. Current status of zirconia restoration. Journal of prosthodontic research, v. 57, n. 4, p. 236–61, 2013. Available on <http://www.sciencedirect.com/science/article/pii/S1883195813000972>. Date of access: 11/8/2015.

MORENO, R. Reología de suspensiones cerámicas, Published by Consejo Superior de Investigaciones Científicas (CSIC), Madrid, 2005.

MUTHUTANTRI, A. I. Novel processing of porous bioceramic structures [tese]. London: University College of London, Department of Mechanical Engineering; 2009. Available on: <http://eprints.ucl.ac.uk/16283/>.

OLIVEIRA, I. R. et al. Dispersão e Empacotamento de Partículas – Princípios e Aplicações em Processamento Cerâmico. São Paulo: Fazendo Arte, 2000. p. 224.

OLIVEIRA, L. Biomateriais com aplicação na regeneração óssea–método de análise e perspectivas futuras. Revista de Ciências Médicas e Biológicas, v. 9, p. 37–44, 2010. Available on:

<http://www.portalseer.ufba.br/index.php/cmbio/article/viewArticle/4730>. .

PARK, J.; LAKES, R. Tissue Engineering materials and regeneration. In: Biomaterials, p. 485–515, 2007. Available on: <http://link.springer.com/chapter/10.1007/978-0-387-37880-0_16>. .

PERKO, S. Moderately porous zirconia ceramics for dental aplications [tese]. Slovenia: Jozef Stefan International Postgraduate School; 2012.

PETSATODIS, G. E. et al. Primary Cementless Total Hip Arthroplasty with an Alumina Ceramic-on-Ceramic Bearing. The Journal of Bone & Joint Surgery, v. 92, n. 3, p. 639-644, 2010. Available on: <http://jbjs.org/content/92/3/639.abstract>. .

PICONI, C., Maccauro, G. Zirconia as a ceramic biomaterial. Biomaterials, v. 20, p. 1–25, 1999. Available on: <http://dx.doi.org/10.1016/B978-0-08-055294-1.00017-9>.

RATNER, B.; HOFFMAN, A. S. A.; SC, D. Biomaterials science: an introduction to materials in medicine. 3 ed. Elsevier; 2013.

SANTOS, D. S. F. Cerâmicas Porosas a Base de Zircônia na Forma de Filmes Suportados Preparados a Partir de Emulsões [Dissertação]. Araraquara: Universidade Estadual Paulista, Instituto de Química; 2015.

SILVA, S. A. Desenvolvimento de elementos sensores do tipo capacitivo composto por filme de cerâmica porosa, com eletrodos integrados, para monitoramento de umidade do ar [tese]. São José dos Campos: Instituto Nacional de Pesquisas Espaciais, Curso de Pós-Graduação em Engenharia e Tecnologia Espaciais/Ciência e Tecnologia de Materiais e Sensores; 2015.

STUDART, A. R. et al. Processing Routes to Macroporous Ceramics: A Review. Journal of the American Ceramic Society, v. 89, n. 6, p. 1771–1789, 2006. Available on: <http://doi.wiley.com/10.1111/j.1551-2916.2006.01044.x>.

THIEME, M. et al. Titanium powder sintering for preparation of a porous functionally graded material destined for orthopaedic implants. Journal of Materials Science: Materials in Medicine, v. 12, p. 225-231, 2001.

TOSOH CORPORATION. Advanced ceramics: Zirconia powders. Available on: < http://www.tosoh.com/our-products/advanced-materials/zirconia-powders>. Date of access: 02/05/2015.

TULLIANI, J. M. et al. Dense and Porous Zirconia Prepared by Gelatine and Agar Gel-Casting: Microstructural and Mechanical Characterization. Ceramic Materials, v. 63, p. 109-116, 2011.

UDUPA, G.; RAO, S. S.; GANGADHARAN, K. V. Functionally Graded Composite Materials: An Overview. Procedia Materials Science, v. 5, p. 1291–1299, 2014. Available on: <http://www.sciencedirect.com/science/article/pii/S2211812814008074>. Date of access: 2/10/2015.

VAGKOPOULOU, T. et al. Zirconia in dentistry: Part 1. Discovering the nature of an upcoming bioceramic. The European journal of esthetic dentistry : official journal of the European Academy of Esthetic Dentistry, v. 4, n. 2, p. 130–151, 2009.

WERR, U. Porous Ceramics Manufacture – Properties – Applications. Ceramic Applications, v. 2, p. 49–53, 2014.

WILLIAMS, D. F. On the nature of biomaterials. Biomaterials, v. 30, n. 30, p. 5897–5909, 2009. Available on: <http://www.sciencedirect.com/science/article/pii/S0142961209007261>.

XIA, C. R.; ZHA, S.; YANG, W.; et al. Preparation of yttria stabilized zirconia membranes on porous substrates by a dip-coating process. Solid State Ionics, v. 133, n. 3, p. 287–294, 2000.

ZHANG, Y.; KIM, J. W. Graded structures for damage resistant and aesthetic all-ceramic restorations. Dental Materials, v. 25, n. 6, p. 781–790, 2009.

ZIELK, H.; ABENDROTH, M.; KUNA, M. Determining fracture mechanical properties for brittle materials using ball on three ball test combined with numerical simulations. Theoretical and Applied Fracture Mechanics, v.86, n. 6, p. 19–24, 2016.

APPENDIX A - Heat treatment on the interval of depositions

The observation, during the first tests, of the thicknesses of the layers produced with more than one immersion led us to believe that the loss of deposited material could be occurring during subsequent immersions; in other words, a layer formed by double dip, would not have necessarily twice the thickness of a layer formed by a single dip. For this reason, an evaluation of the best procedure between immersions was made to avoid loss of the first deposited material during the subsequent immersion.

It was analyzed that double-dip layer, formed by Z40 followed by Z70, would make it possible to visualize the “row” of different particle sizes, and the total thickness of the final layer. Between the dips, three steps were tested: 1 - air flow (drying by air), 2 - pre-sintering (1150ºC) and 3 - sintering (1500ºC). Figure A.1 shows the formed layers, with the average final thickness indicated on each case.

Although there was no substantial difference on the thickness of tested conditions, the images show a higher value to the "pre-sinter" amid layers condition, which indicates a lower material loss during subsequent immersion than the “air dryer” condition. The sintering step among immersions could induce a great reduction of the sphere sizes, leading to crack the layers. In this way, it was decided to “pre-sintering” the samples on every interval of subsequent deposition.

Figure A.1 - Effect of heat treatment on the final thickness of layers form by two immersions: Z40 followed by Z70: (a) air dryer, (b) 1150°C (no plateau), and (c) 1500°C (no plateau).

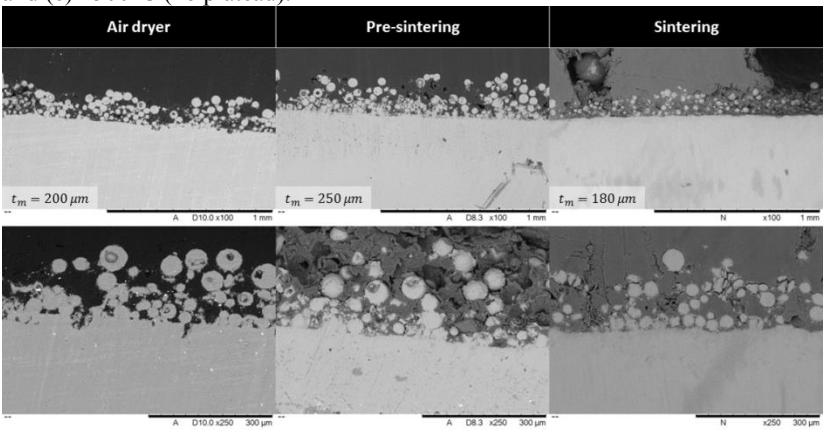

APPENDIX B - Porous solids

The idea of production of porous solids emerged to estimate values of porosity and resistance of the layers produced by dip coating, once there was no way to evaluate those properties in such a thin part. As discussed along the work, the morphology of these solids were not equivalent to the deposited layers via dip coating, as seen in the images below. Despite morphologic differences, the mechanism used to form those solids is basically the same used on dip coating, in a way that particles are conformed almost in absence of external forces, what enables an approximation of properties of both materials (made by slip casting and dip coating).

Most specimens showed good distribution between fine and coarse particles, but some of them presented spots of agglomerate fine particles. The increase of Z3 amount was not evidenced in all images of porous solids; the heterogeneity of the specimens does not allowed a pattern of morphology in different situations. In the comparison between porous solids (slip casting) and deposited layers under the same condition (amount of Z3), the “binder mass” was more visible in the first case, possibly due to a gathering of particles near external faces, formed during drying.

Figure B.1 - Porous solids made with Z40 powder plus 5% Z3 (left) and 15% Z3 (right).

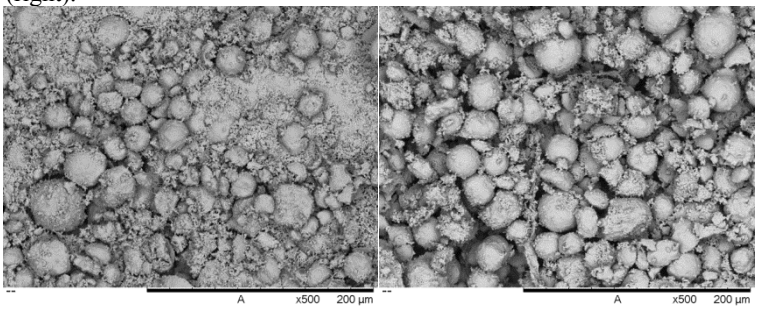

Figure B.2 - Porous solids made with Z70 (left) and Z100 (right), both with 25% Z3.

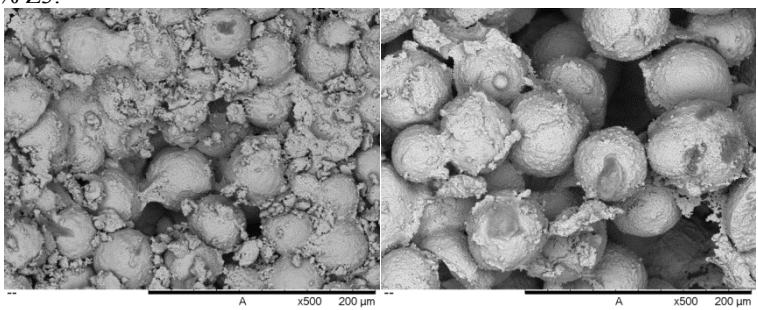

APPENDIX C - Delamination and defects on deposited layers

Several defects occurred during experiments. The first trace of delamination appeared after pre-sintering of a single-dipped specimen, with a detached layer that indicates drying issues. From this evidence, the pieces began to pass through air-drying before undergoing pre-sintering (or sintering) step. After B3B bending tests, this problem was again evidenced with a slight difference: the detachment occurs between layers, not between layer and substrate as seen it before. Figure C.1 (left) shows part of the layer adhered to the substrate, illustrating the described situation on a double-dipped Z40 layer; the right image also contains parts of an adhered layer, near the fracture surface. The thicker the layer, the higher frequency of delaminations was observed, suggesting a possible relation of the defects with the successive exposure to thermal treatments (among dips).

Figure C.1 - Example of delamination of the double-dipped Z40 layer, after flexural test. Left: cross-section view. Right: top view of the fracture surface.

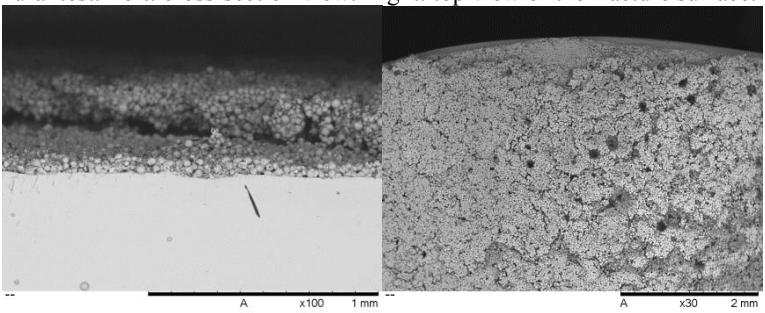

Bubbles and thickness variations were also common defects along experiments, both observed in Figure C.1 (right). The emergence of bubbles is associated with the suspensions conditions: the tendency of suspensions to become more viscous as reused after a few days, due to loss of water, favored bubble's formation.

In some layers produced with larger particles, Z70 and Z100, small islands of fine material were formed, as can be seen Figure C.2. To avoid such heterogeneity, constant stirring of suspensions was required in the immersion intervals.

Figure C.2 - Heterogeneous surface: isles of fine particles and/or lack of coverage of the substrate. Up: Z70 - 1 dip; down: Z100 - 1 dip.

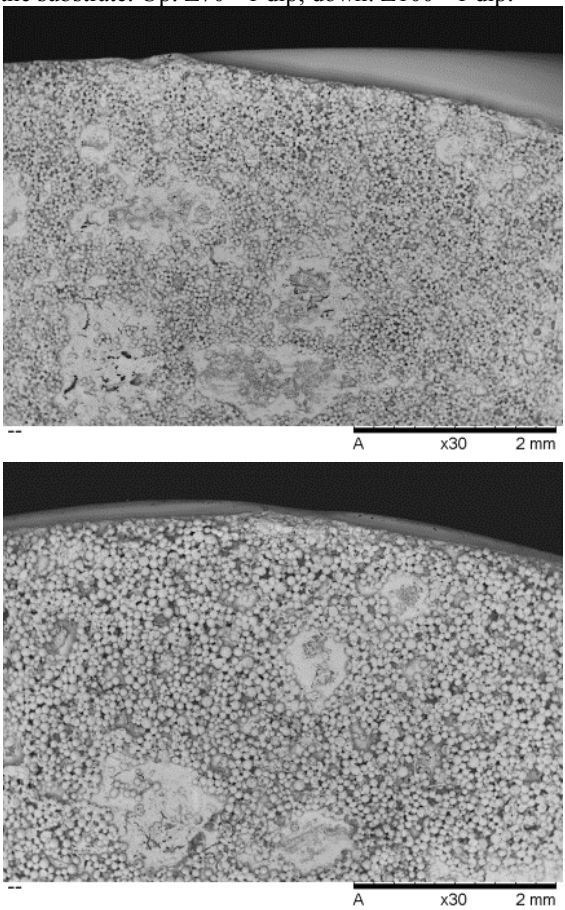

The presence of hollow spheres did not prove to be a problem in the processing, nor in the porosity, but it was observed with great frequency in the analysis of the layers, being a defect coming from the manufacturer.

Figure C.3 – Sintered hollow spheres.